C Journal of Carbon Research

MDPI

Review

An Overview of the Recent Progress in the Synthesis and Applications of Carbon Nanotubes

Gul Rahman [1,*], Zainab Najaf [1], Asad Mehmood [2], Salma Bilal [3], Anwar ul Haq Ali Shah [1], Shabeer Ahmad Mian [4] and Ghulam Ali [5]

1 Institute of Chemical Sciences, University of Peshawar, Peshawar 25120, Pakistan; zainabnajaf110@yahoo.com (Z.N.); anwarulhaqalishah@uop.edu.pk (A.u.H.A.S.)
2 Department of Energy and Materials Engineering, Dongguk University-Seoul, Seoul 04620, Korea; asad_qau@hotmail.com
3 National Center of Excellence in Physical Chemistry, University of Peshawar, Peshawar 25120, Pakistan; salmabilal@uop.edu.pk
4 Department of Physics, University of Peshawar, Peshawar 25120, Pakistan; shabeerahmad@uop.edu.pk
5 Center for Energy Convergence Research, Korea Institute of Science and Technology (KIST), Hwarang-ro 14-gil 5, Seongbuk-gu, Seoul 02792, Korea; Ali@kist.re.kr
* Correspondence: gul_rahman47@uop.edu.pk; Tel.: +92-91-911-6652

Received: 13 October 2018; Accepted: 27 December 2018; Published: 3 January 2019

Abstract: Carbon nanotubes (CNTs) are known as nano-architectured allotropes of carbon, having graphene sheets that are wrapped forming a cylindrical shape. Rolling of graphene sheets in different ways makes CNTs either metals or narrow-band semiconductors. Over the years, researchers have devoted much attention to understanding the intriguing properties CNTs. They exhibit some unusual properties like a high degree of stiffness, a large length-to-diameter ratio, and exceptional resilience, and for this reason, they are used in a variety of applications. These properties can be manipulated by controlling the diameter, chirality, wall nature, and length of CNTs which are in turn, synthesis procedure-dependent. In this review article, various synthesis methods for the production of CNTs are thoroughly elaborated. Several characterization methods are also described in the paper. The applications of CNTs in various technologically important fields are discussed in detail. Finally, future prospects of CNTs are outlined in view of their commercial applications.

Keywords: carbon nanotubes; synthesis routes; biomedical applications; energy storage and conversion; electronic devices

1. Introduction

Carbon is an astonishing element, not only due to the reason that it is the element necessary for all life processes, but also because of the fact that it can occur in various allotropic forms [1]. Conventionally, carbon materials consist of graphite blocks, the category under which activated carbons, carbon blacks, and diamonds are present. The recently developed materials of carbon include nanotextured and nanosized carbons. Nanotextured carbons cover a large variety of carbon structures, from carbon fibers, pyrolytic carbons, or glass-like carbons, to diamond-like carbon materials. The nanosized carbons (or nanocarbons) comprise fullerenes, graphene and CNT [2]. Extraordinary importance is given to graphene and CNTs, as they play a vital role in current advances based on nanomaterials, including conductive and high-strength composites [3], artificial implants [4], drug delivery systems [5], sensors [6], energy conversion and storage devices [7], radiation sources [8] and field emission displays [9], hydrogen storage media [10] and nanometer-sized semiconductor devices [11], probes [12], and interconnects [13]. Radushkevish and Lukyanovich first detected and described CNTs in 1952 [14], and later, the SWCNTs were observed by Oberin

in 1976 [15]. The discovery of CNTs in recent history is ascribed to Iijima, who for the first time, described multi-walled carbon nanotubes (MWCNTs) in carbon soot obtained during C_{60} carbon molecule fabrication in an arc evaporation test [16]. CNT is a beehive-shaped tube, having unique 1D nanostructures with carbon atoms belonging to sp^2 hybridization. They have a thickness of approximately 1/50,000th of human hair. CNTs exist in three unique geometries, which are armchair, zig-zag, and chiral (Figure 1). The mechanical, electrical, optical, and other properties of CNTs are determined by the chirality. It has been reported that the electrical properties of CNTs are influenced by the chiral vector and corresponding pairs of integers [17]. Depending on rolling up of the graphene sheets, CNTs can be either narrow-band semiconductors or metals [18]. Thus, some nanotubes behave more like silicon, while others show higher conductivities than that of copper.

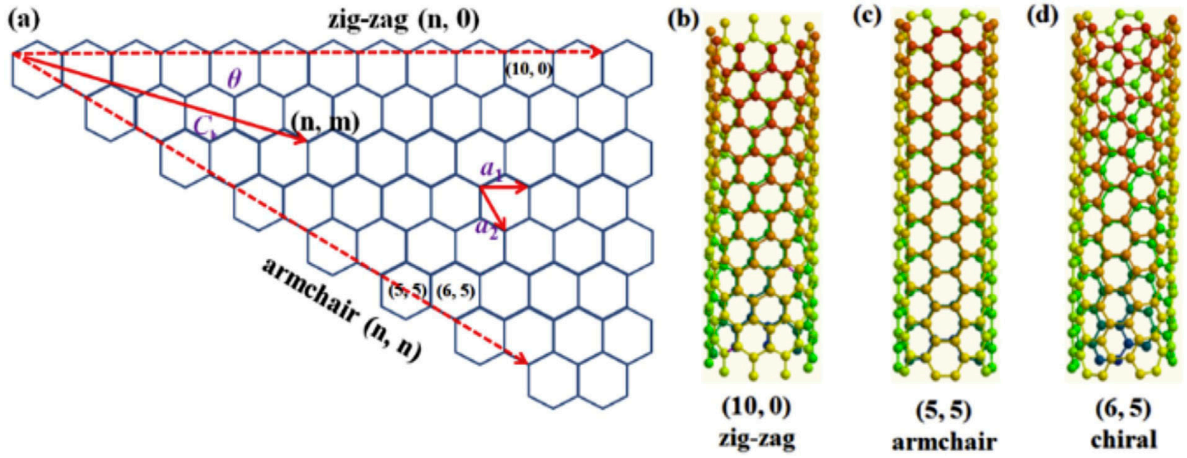

Figure 1. Geometries of CNTs. Reproduced with permission from [19]. Copyright Elsevier, 2016.

Taking into account the number of layers of CNTs, they may be single-walled carbon nanotubes (SWCNTs) or multi-walled carbon nanotubes (MCWNTs) (Figure 2). Most SWCNTs have a diameter extending from 0.4 to >3 nm, whereas the length can extend to a few millions times the diameter. Conceptualizing the wrapping of a layer of graphene into the shape of a tube gives the structure of SWCNTs, while multiple rolled layers (concentric tubes) of graphene constitute MWNTs. In MWCNTs, the interlayer space is approximately equal to the space between the graphene sheets in graphite, which is 3.4 Å. The diameter ranges from 1.4 to at least 100 nm for MWCNTs [20,21].

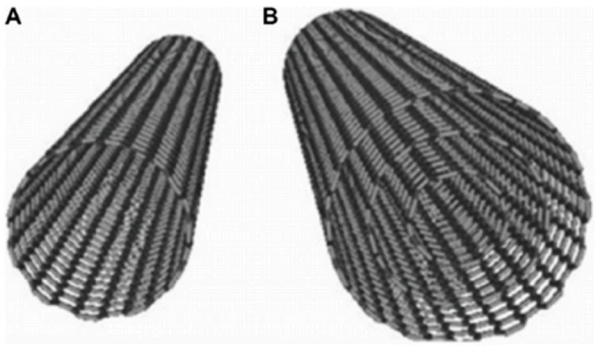

Figure 2. (**A**) Structure of SWCNT; (**B**) MWCNT. Reproduced with permission from [22]. Copyright DOVE Medical Press, 2016.

Table 1 compares the key differences between the SWCNTs and MWCNTs [23]. The morphologies of CNTs affects their optical properties, thermo-physical characteristics, and photo-thermal conversion abilities [24].

Table 1. Comparison between SWCNTs and MWCNTs [23].

SWNT	MWNT
Single graphene layer	Multiple graphene layers
Synthesis requires catalyst	No catalyst is required
Difficult bulk synthesis due to the requirement of appropriate growth and atmospheric condition.	Easy bulk synthesis
Poor purity	High purity
Greater chances of defects during functionalization	Lesser defect chances but when this occurs, it is hard to recover
Aggregation in the body is less	Aggregation in the body is greater
Easy assessment and characterization	Structure is complicated
More pliable and easily twisted	Twisting is not easy

2. Synthesis of CNTs

For the synthesis of CNTs, various routes can be employed to fabricate CNTs of desired properties that are needed for a particular application. Generally, those methods are preferred, which produce CNTs having less structural and chemical imperfections. In this section, different methods for the synthesis of CNTs are briefly overviewed.

2.1. Arc Discharge Method

The arc discharge method is a well-known method for the formation of CNTs. Figure 3 illustrates the schematic diagram of Arc discharge method. In this method, a buffer gas such as helium is introduced in a chamber containing a cathode, a graphite anode, and vaporized carbon molecules. The chamber also contains a small amount of metal catalysts such as nickel, cobalt or iron. Under applied pressure, the chamber is heated to 4000 K, and a direct current (DC) current is passed through the sample. In the progression of this technique, nearly half of the vaporized carbon solidifies on the tip of cathode in the form of a "hard cylindrical deposit". Condensation of the remaining carbon occurs, forming "cathode soot" on the cathode, and "chamber soot", which is present all over the walls of the chamber (Figure 3). The chamber and the cathode soot yield either SWCNTs or MWCNTs. The selection of the inert gas and the added metallic catalyst decides whether the resultant CNTs are SWCNTs or MWCNTs [25]. For the production of SWCNTs, catalyst precursors are necessary for growth in the arc discharge, while the anode is immersed with a metal catalyst, such as Fe, Co, Ni, Y, or Mo [26]. Studies have revealed that SWCNTs with a diameter of 1.4 nm can be synthesized by Ni-Y graphite mixtures, giving yields of <90% [18]. This mixture is nowadays used worldwide for the fabrication of SWCNTs at high yield. The advantage of this method is the high yield of nanotubes. However, the little control over the orientation of the nanotubes is the key disadvantage that ultimately affect their activity. Furthermore, due to the involvement of a catalyst in the production of SWCNTs, the products need to be purified later on [25]. Methods such as centrifugation, oxidation, filtration, and acidic treatment are being used for the purification [27].

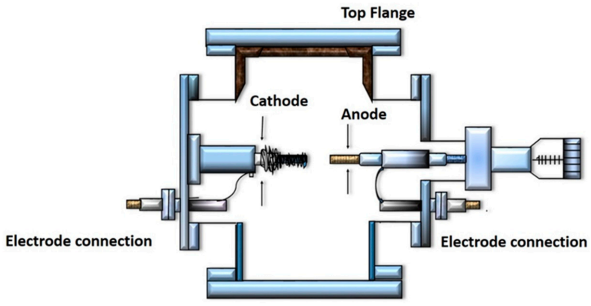

Figure 3. Schematic diagram showing the Arc discharge method.

The generation of arc-discharge in liquid nitrogen can be used for the production of MWCNTs under low pressure, without costly inert gases [28]. The magnetic field synthesis method can be used to control the arc discharge for the synthesis of CNTs, and the produced CNTs have purities >95% (Figure 4) [29].

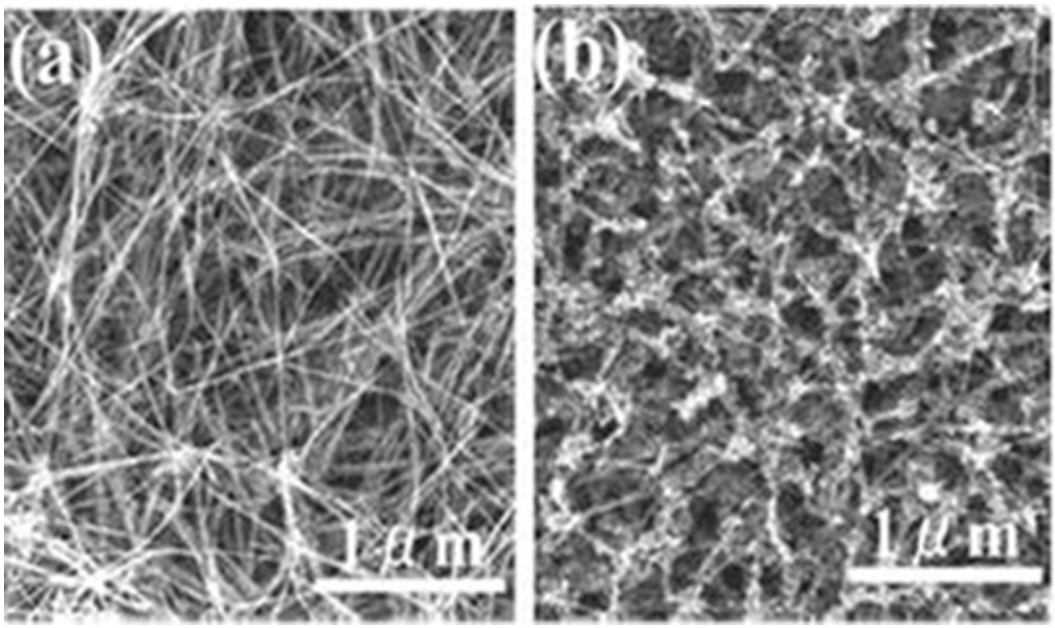

Figure 4. SEM images of MWCNTs (**a**) in the presence of and (**b**) in the absence of a magnetic field. Reproduced with permission from [29]. Copyright AIP, 2002.

Moreover, large-scale synthesis is achieved by plasma rotating arc discharge (Figure 5). In this technique, a plasma rotating electrode process is involved, to solve the problem of the non-uniform cathode surface and the co-existence of impurities with the CNTs in the conventional arc discharge technique. CNTs are synthesized by the rotation of the graphite rod with a high velocity. Centrifugal force is produced by rotation, which in turn creates turbulence and causes an acceleration of carbon vapor that is perpendicular to the anode. The carbon vapor does not condense at the surface of cathode, but is collected on the graphite collector that is located at the boundary of the plasma. The collector becomes closer to the plasma as the speed of rotation increases, and the yield of CNTs is also increased [26].

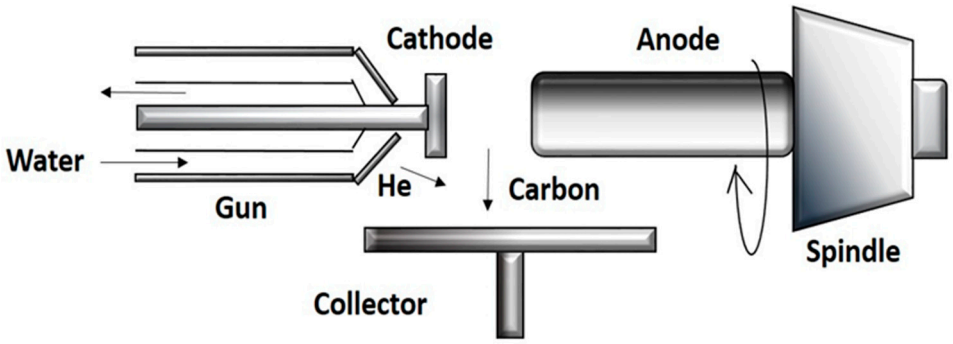

Figure 5. Schematic diagram showing rotating arc discharge.

2.2. Laser Ablation Method

The laser ablation technique and the arc discharge method are similar in principles and mechanisms; however, they are different by the input energy sources. In the laser ablation method,

the required energy is provided by a laser. Figure 6 shows the schematic structure of an experimental setup. A tube made up of a quartz-containing graphite block is heated in a furnace at 1200 °C, using a high-power laser in the presence of metal particles as catalysts [25]. A stream of argon is maintained during the course of the reaction. The graphite within the quartz is vaporized by a laser. Argon carries away the vaporized carbon, which condenses downstream onto the cooler walls of the quartz. SWCNTs and metallic particles are present in this condensation. According to studies, the laser power can influence the diameter of the CNTs. The diameter of the tube becomes thinner as the laser pulse power is increased [30]. Other studies reported that ultrafast laser pluses are of great potential, and are capable to produce larger quantities of SWCNTs [31]. The SWCNTs produced by this method are of high purity and quality. The position where the carbon atom starts to condense should be set up as a curved sheet of graphene with a metal catalyst atom nearby for the proper fabrication of the condensed nanotubes. When carbon atoms begin to assign for the formation of rings, the proper electronegative properties of the metallic atom prevent the open edge from closing [25]. The main advantages of this technique include relatively low metallic impurities, and a relatively high yield, due to the vaporization tendency of the metallic atoms from the end of the tube, once it is closed. The key drawback of this technique is that the synthesized nanotubes may not be regularly straight, and have some degree of branching. Furthermore, this procedure involves graphite rods of high purity, and requires high powers of lasers, and the amount of CNTs produced are not as great as in the arc-discharge technique.

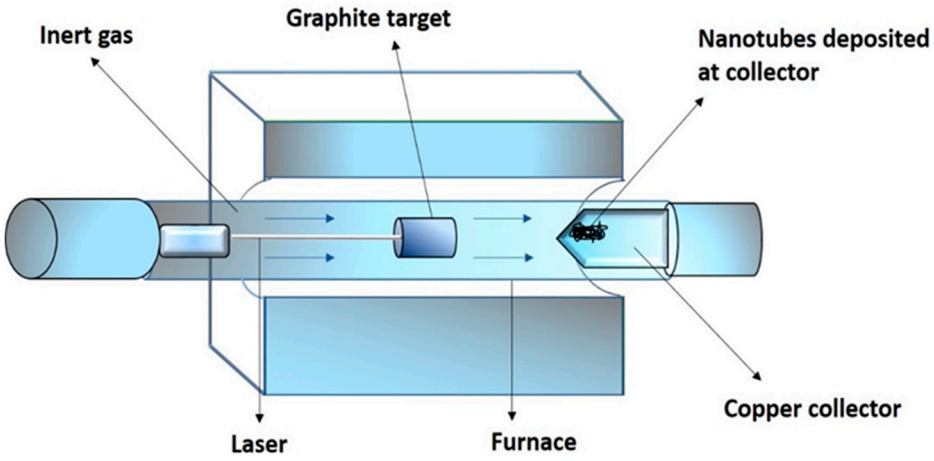

Figure 6. Schematic structure showing the laser ablation method.

2.3. Chemical Vapor Deposition (CVD)

CNTs can be grown on a variety of materials by the CVD approach, and this makes it more viable to participate in ongoing processes for manufacturing electronics. This method can be further classified into various types, including CCVD (catalytic chemical vapor deposition) [32], PE-CVD (plasma-enhanced chemical vapor deposition) [33], microwave plasma (MPECVD) [34] and oxygen-assisted CVD. The experiment is mostly performed at atmospheric pressure in a flow furnace. The modality of the furnace is of two types. In one type, there is a horizontal configuration, and in another, there is a vertical configuration. The application of the horizontal furnace is dominant. The catalyst here is implanted in a quartz or ceramic boat, which is planted into a quartz tube. The reaction mixture consists of an inert hydrocarbon, and a source of hydrocarbon. This mixture is passed through a catalyst bed at temperatures in a range of 500 °C to 1100 °C. Afterwards, the temperature of the system is cooled to room temperature. The vertical configuration of the furnace is typically implemented in the sustained mass production of carbon nanotubes/fibers. The carbon source and catalyst, are both introduced at the topmost part of the furnace. The resultant filaments build up throughout the flight, and then are accumulated at the lower portion of the chamber. Ultrafine metal catalyst particles are inaugurated either directly to the reactor, or are manufactured in situ,

utilizing precursors like metallocenes [35,36]. The typical growth mechanism of nanotubes in the process of CVD includes the catalyzed dissociation of hydrocarbon molecules by the transition metal and saturation of carbon atoms in the metal nanoparticle. The metal particle precipitates out carbon, which leads to the generation of tubular carbon solids with sp^2 structure. The characteristics of CNTs manufactured by the CVD technique is dependent on the working conditions, for instance, the operation pressure, temperature, hydrocarbon concentration, the nature of the support, and the kind and the time of reaction [37]. The diameter of the nanotube can be controlled by altering the active particles on the catalyst surface. The time of the reaction is responsible for the length of the tubes; even long tubes of up to 60 mm can be produced [38]. Commonly used metal catalysts are Ni, Co, Fe, or their combinations, as Ni-Y, Fe-Ni, Co-Ni, etc. [25,39,40] while regarding the carbon source, the most favored in CVD are hydrocarbons like methane, acetylene, ethane, ethylene, xylene, or eventually their mixture, ethanol, or isobutane. The SWCNTs, with diameters of approximately 3.23 nm, have been effectively synthesized by Yang et al., via the catalytic decomposition of a hydrocarbon with helium and hydrogen as the carrier gases [41,42]. Zhang et al., synthesized MWCNTs with diameter of 40–60 nm by the catalytic decomposition of methane at a temperature of about 680 °C for 120 min, using catalyst nickel oxide–silica binary aerogels [43]. This process enables the selective growth of CNT in many forms, e.g., powder [44] and the aligned forest of the CNTs [45,46]. The tubes that are produced can acquire several shapes, i.e., they can be made straight, helix, planar-spiral, or curved, often with striking constant pitch. This technique is advantageous because the purity and yield is very high, the alignment of the CNTs is regular, and the reaction course is easy to control [47].

2.4. Flame Synthesis Method

Flames offer the potential for the fabrication of CNTs in large amounts at considerably lower cost, as compared to the existing methods. It is capable of producing nanotubes of carbon on required surfaces, and specifically in a controllable way. There are three essential constituents that are necessary for the production of CNTs. These are: metallic catalyst particles, a heat source, and a source of carbon. The catalytic precursors, in the flame synthesis method are usually introduced into the flame system, where they undergo nucleation and finally condense into solid spherical metallic nanoparticles. Flame parameters can also be applied to obtain suitable flame conditions, which would enable the fabrication of ideal sizes of catalyst particles for the growth and inception of CNTs. The catalyst properties and alteration of the flame parameters can remarkably influence the heat and carbon source, the activation and deactivation of catalyst particles, and the formation of catalysts, as well as the morphology of the final synthesized products [48]. As a consequence, several flame patterns, including premixed, partially premixed, and inverse diffusion flames, have been used for the production of CNTs and nanofibers [49,50]. For the fabrication of MWCNTs, Yuan et al. [51,52] assessed the effects of fuel type, type of catalytic support, residence time, and its delivery method by using a laminar co-flow diffusion flame. Experiments carried out by Lee et al. [53] revealed that the temperature of the flame play a vital role in the fabrication and alignment of CNTs. Similarly, the formation of SWCNTs in a controlled flame environment can be carried out, using hydrocarbon fuels and small aerosols of metal catalysts [54,55]. The flame-assisted fabrication of SWCNTs is difficult, as it involves the introduction of the catalyst in the gaseous phase, to obtain the ultra-small catalyst particles that ideal for the inception CNTs. SWCNTs have been detected in the post-flame region of a premixed acetylene/oxygen/argon flame operated at 50 Torr (6.7 kPa), using the vapor of iron pentacarbonyl as a source of metallic catalyst, Nanotubes are observed to combine and form masses of between 40 and 70 mm, above the burner (~30 milliseconds) [56].

2.5. Saline Solution Method

Using a saline solution method for the production of CNTs, a stainless steel mesh or carbon paper is used as a substrate, which is submerged in a saline solution of a metal catalyst, preferably Co:Ni, in a 1:1 ratio, and a carbon containing a gas source such as ethylene is passed through the substrate.

An electrical current is applied for heating the substrate. As a result, a reaction takes place between the gas and catalyst, to yield CNTs supported on the conductive substrate [57].

2.6. Spray Pyrolysis Method

Spray pyrolysis is a favorable technique for the production of CNTs on different surfaces. This method is a modified form of the CVD method. Using spray pyrolysis (or injection CVD) technique, high purity MWCNTs can be obtained by using different aromatic and aliphatic hydrocarbons and ferrocene as a catalyst precursor [57]. In this technique, the system is well sealed to prevent leaking. The system uses a thermolyne single zone split tube furnace with a quartz tube. A vacuum tight assembly is built for the solution. Samples are placed on a quartz or stainless steel boat, which is about nine inches from the center of the tube furnace. Pure argon is introduced in the quartz tube reactor. The furnace is heated in the presence of argon flow (50 sccm). When the injector head reaches 170 °C, the argon flow rate is increased to 100 sccm, and the mixture of ferrocene dissolved in xylene is rapidly injected until the solution reaches the injector head. This results in the production of black CNTs powder, which are collected [58]. The product is washed with HNO_3 (40 wt. %) to remove the catalyst particles and amorphous carbon [59]. The key advantage of this technique over other CVD methods is that the catalyst precursor and the liquid hydrocarbons, can be introduced continuously into the reaction zone; hence, making the production of MWCNTs cheaper and semicontinuous [60]. Additionally, it offers the injection of liquid additives into the reaction cavity in an easy and controlled way.

3. Characterization Techniques for CNTs

3.1. Raman Spectroscopy

The Raman experiment is a quick, simple, non-invasive, and non-destructive characterization technique. It can be carried out at room temperature and pressure, and the instrumentation is mostly accessible to a wide range of user communities [61]. This technique is extremely sensitive for examining the changes in the nanotubes properties synthesized using various procedures and conditions. The Raman signal intensity for the sample increases with the incident laser power, providing detailed and precise electronic and structural characterization [62]. There are two principal Raman features comprising the low frequency radial breathing mode (RBM) and multi-feature tangential (G band), found at relatively greater frequencies. Some other weak features observed are the iTOLA band (optical and acoustic modes combination), D band (disorder induced), and the M band (an overtone mode). The intermediate frequency modes (IFM) are detected in the Raman spectrum by increasing the background intensity. These modes are observed in between the RBM and G-band features [63]. The diameter of the nanotube (dt) can be studied by using the RBM. The Raman feature (RBM) relates to the C atom vibration in the radial direction, and the tube seems to be "breathing". These features are distinctive to CNTs. Therefore, RBM frequencies are advantageous for detecting whether a particular carbon material comprises of SWCNTs or MWCNTs. The diameter of CNTs can be determined in the presence of RBM modes, using the relation:

$$\mathrm{RBM} = \mathrm{A}/\mathrm{dt} + \mathrm{B},$$

where the A and B are the parameters determined experimentally [64,65]. Furthermore, the electronic structure can be examined by using the resonance Raman intensity (I_{RBM}). The electronic states available for the optical transitions mainly influences the I_{RBM} [66]. In most graphitic materials, the G-band usually seems as a single peak, but sometimes (at the distinct nanotube level), two-peak structures appear, for both semiconducting [67] and metallic [68] nanotubes. The doublet G-band structure detected in 3D graphitic materials is ascribed to the interlayer coupling [69], while this phenomena does not appear in the case of SWCNTs. Moreover, variations in the D- and G-band can be used to investigate and display structural changes in the sidewalls of the nanotube that arise, due to

the addition of different chemical species and the introduction of defects. In addition, overtones and the combination modes above the G-band frequency are rare, due to dispersion effects that make these features broad and too weak to pick out from the noisy background. However, such combination modes and overtones are clearly observed in SWCNTs, due to double resonance phenomena and the occurrence of van Hove singularities [66].

3.2. Transmission Electron Microscopy

Transmission electron microscopy (TEM) is used to study thin specimens, by the generation of a projection image through the passage of electrons. TEM is similar to the conventional (compound) light microscope in many ways [70]. TEM images can be used to measure the diameters of one CNT, as well as CNT bundles. The smallest diameter of SWCNT bundles is approximately 4 nm, and all of the DWCNTs show diameters of greater than 2.5 nm. High-magnification TEM images also allow statistical measurements of the spacing between fringes in several bundles [71].

3.3. Atomic Force Microscopy

The atomic force microscopy (AFM) is the most extensively used characterization technique amongst the present microscopy techniques. The extensive use of the AFM is ascribed to three-dimensional sample topography with atomic resolution within a short time, for a comparatively low cost [72]. Additionally, essential information related to the structural investigation of the surface is covered by the AFM data. This technique also gives us information about the length of the nanotubes, and an approximate valuation of the diameter of the bundles [71].

4. Shapes of CNTs

Various morphologies of CNTs have been synthesized and observed, which include waved, straight, coiled, branched, beaded, and regularly bent structures. Substrates of porous silicon are also used to produce MWCNTs that are grown perpendicular to the substrate [46], giving them a straight structure (Figure 7). Millimeter-high SWCNT arrays were first effectively fabricated by Hata et al. [73] via water-assisted CVD but the most effective method is direct growth by using a catalytic CVD method, with the intervention of external forces [74,75]. These forces can be produced by an electric field [76], gas flow [77,78] or surface interactions of the substrate [59,79]. Well-arranged horizontal CNT arrays on appropriate substrates are greatly preferred in field-effect transistors [80], light emitters [81], and logic circuits [82]. Moreover, the proper combination of the external forces is an approach to synthesize regularly bent CNTs, which are produced via a DC plasma-enhanced CVD method [83]. Changing the direction of electric field lines causes the regular bending of CNTs. These CNTs are suggested for applications comprising high-resolution AFM tips, mechanical nano-spring devices, and nano-circuit interconnections in devices [84]. In the absence of an external force, a single nanotube may bend during growth, giving rise to waved CNTs (Figure 8). This bending, in principle, can arise from a topological pentagon–heptagon defect pair, or the internal mechanical deformation under slight bending stress, which can be caused, due to the nanotube's own weight, inadequate growing space, or interaction with the surrounding nanotubes [85,86].

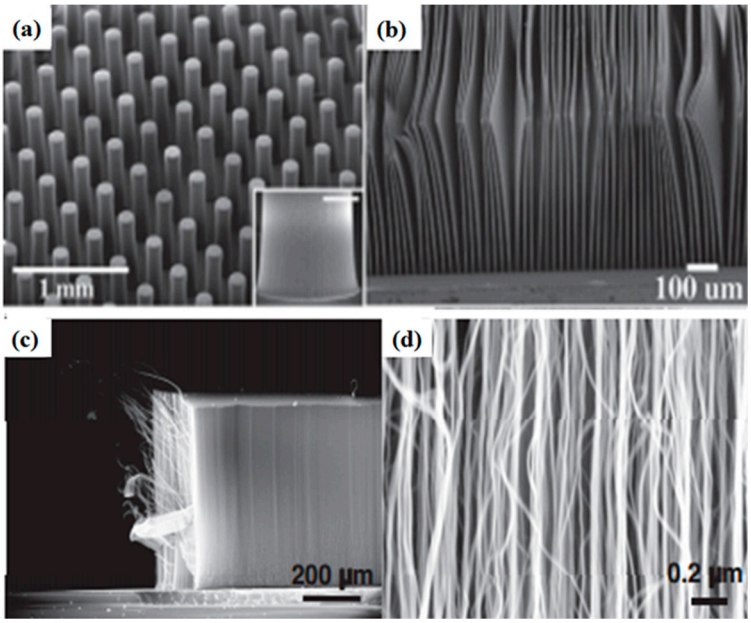

Figure 7. (**a**) SEM micrograph of cylindrical pillars of SWCNTs; (**b**) SEM images of 10 µm thick SWCNT sheets. Reproduced with permission from [73]. Copyright AAAS, 2004. (**c**,**d**) super-aligned MWNT array with different magnifications. Reproduced with permission from [84]. Copyright Elsevier, 2009.

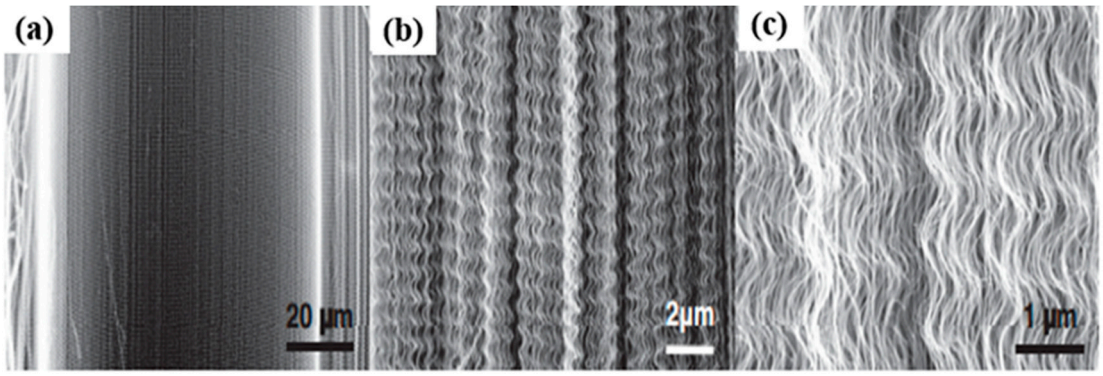

Figure 8. SEM images of a MWNT array with wavy structures at various magnifications (**a**–**c**). Reproduced with permission from [84]. Copyright Elsevier, 2009.

Furthermore, helically coiled shape CNTs consisting of pentagon–heptagon paired atomic rings have been reported in literature (Figure 9) [87].They were first detected in the 1990s [88,89]. They can be synthesized in large amounts by catalytic CVD [90–93]. The unusual morphology of coiled CNTs impart them some functionalities such as the high-efficiency of electromagnetic wave absorbers capacity, electrical inductors, resonators, sensors, nanostructured mechanical springs, and magnetic beam generators [84,94].

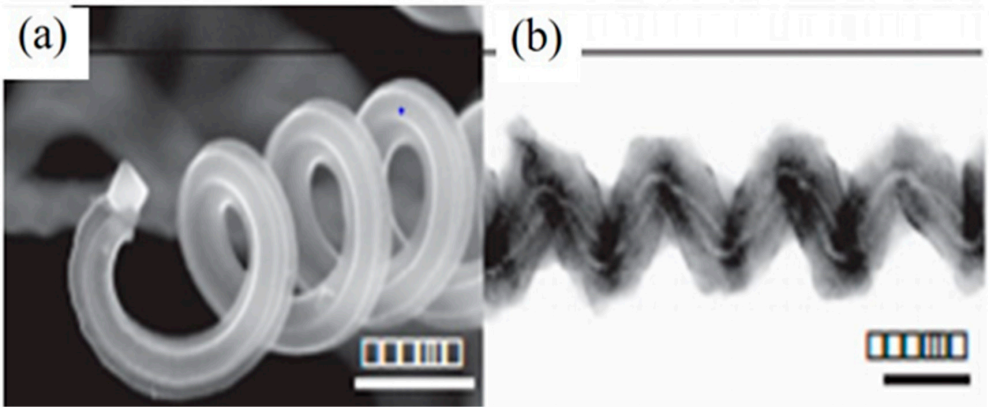

Figure 9. SEM image of helically coiled CNTs (**a**) Tip of a coil. The scale bar is 600 nm; (**b**) TEM image of two tubules, forming a coil with different diameters, but the similar pitch, and a small alteration in phase. The scale bar is 100 nm. Reproduced with permission from [84]. Copyright Elsevier, 2009.

CNTs are also found in branched structures resembling letters L, Y, T, and more complex connections which were firstly detected in nanotubes synthesized by arc-discharge [95]. The CNT Y-connections are made by the decoration of hexagonal network with non-hexagonal rings, where the three outlets of the Y are joined [96,97]. The initial synthesis was figured out in Y-shaped templates by acetylene pyrolysis in the year [98]. Branched SWCNTs are understood to have an extreme control on electronic devices, as they can be used as nano-transistor, nano-diode, and nano-interconnect in nano-electron devices [84]. CNTs with beads have been obtained in different processes [15,99–104]. Beads appear in different forms, and they may have either polycrystalline or amorphous graphite. Their formation is due to the increase in the viscosity of viscous carbon on the nanotube surface, and deterioration of beading process upon the cooling process. As shown in Figure 10, the nanotube can be clearly seen inside the bead. Such CNTs are likely to be used in composites as fillers to improve matrix material electrical conductivity, and mechanical strength, due to the reason that the beads prevent the nanotubes from slipping in the composite materials [84].

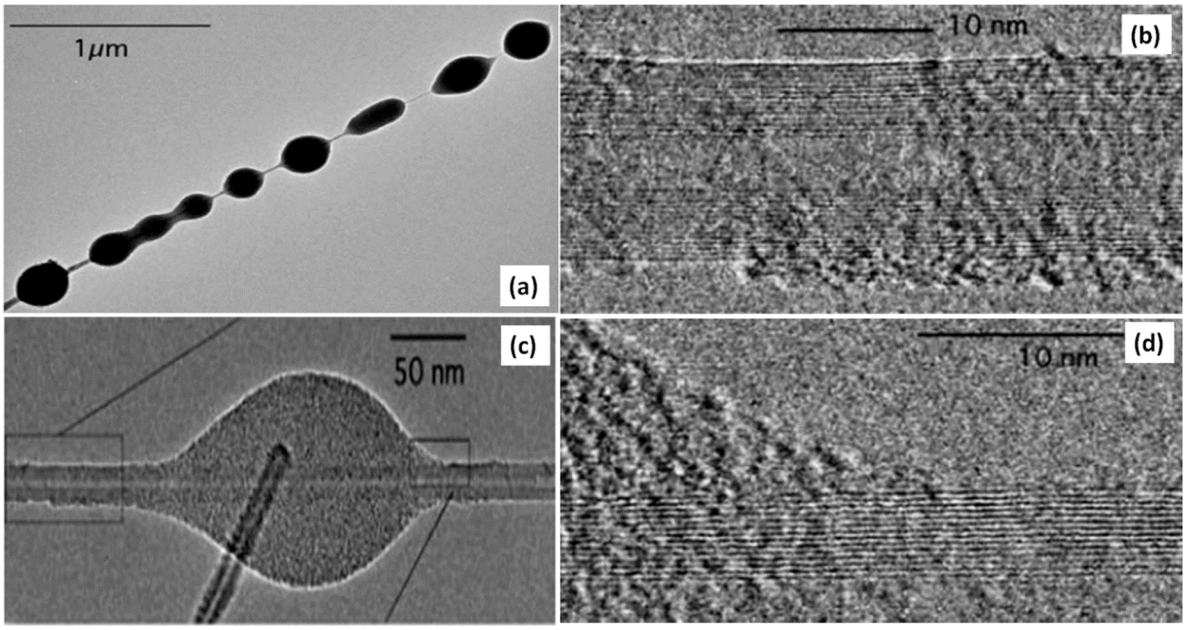

Figure 10. (**a**) TEM image of a MWNT with many beads; (**c**) TEM image of a small, elongated bead on MWCNT of 15 layers; (**b**,**d**) High-resolution TEM images of the beads. Reproduced with permission from [100]. Copyright AAAS, 2005.

5. Applications of CNTs

Applications of CNTs could take along many environmental and health benefits, owing to their superior performance. CNTs have outstanding electronic [105], optical [106], thermal [107], chemical, and mechanical characteristics [108,109]. The best known thermal conductor prior to CNT was diamond. But the thermal conductivity of CNTs is at least twice that of diamond [110]. The extraordinary mechanical strength of the CNTs is due the sp^2 carbon-carbon bonding [111]. The nanotubes exhibiting a high mechanical strength with a Young's modulus value of 1000 GPa, (approximately five times higher than that of steel), are considered the best for a variety of applications [112]. CNTs can have a breaking strain or tensile strength of approximately 63 GPa, which is about 50 times greater, compared to that of the steel [113]. CNTs have extraordinary electrical properties, due to their peculiar electronic structure and the 1D character of graphite. Their electrical resistance is extremely low, because resistance occurs when an electron in the crystal structure collides with some defect in the material through which it is passing, but electrons are not easily scattered in CNTs [114]. The construction of nanoscale electronic devices from nanotubes is of great interest, and some advancement is being made in this area. However, for the construction of a useful device, thousands of nanotubes are needed to be arranged in a defined pattern. Carbon nanotubes, due to their incredible properties, find applications in many fields. However, nanoparticles tend to agglomerate in base fluids, due to their hydrophobic nature and strong Van der Waals inter-particle interactions, which is a major technical barrier [115]. The most important challenge is the high dispersion and stability of CNTs in aqueous media [116]. Different properties like absorption, viscosity, and thermal conductivity are affected by the stability of CNT [117,118]. To overcome this problem, the functionalization of CNTs is usually carried out [119]. By this way, it is possible to disperse the CNTs in water, which opens the route for their easy processing in physiological environments [26]. In vitro studies have indicated that the intrinsic toxicity of SWCNT, functionalized by phenyl–SO_3H or phenyl–$(COOH)_2$ groups by a covalent method decreases the cytotoxic effects [120]. Some of the applications of CNTs are revised in this section.

5.1. Energy Storage and Conversion

Due to the increasing global energy demand, nature is being relentlessly investigated by humans to make use of existing resources of energy. Whether renewable or non-renewable, nearly all of the promising substitutes are examined and utilized [121]. There is a great demand of cost-effective and reliable technologies for a sustainable production and the storage of electrical energy for various applications, including transport and portable devices [122]. Solar energy is thought to be the solution for the increasing energy demand, as it is an abundant and sustainable source of energy [123]. Generally, solar energy can be harvested as solar electric conversion and solar thermal conversion [124]. However, the main limitation of solar collectors is the low efficiency of thermal conversion. Carbon nanofluids are extensively used in the solar thermal conversion, due to their excellent performance as a solar absorber and a heat transfer fluid [125]. It has been shown that the performance of potassium persulfate-treated MWCNTs in therminol55 (K–MWCNTs–TH55) dropped at a considerably higher temperature, as compared to the untreated TH55, which suggests that K–MWCNTs–TH55 absorb sunlight more efficiently than TH55. Recently, stable CNT fluids have attracted the attention for use in direct absorption solar collectors (DASCs) [24]. In solar thermal conversion systems, the nanofluids have outstanding potential as heat transfer fluids [126]. The modification of MWCNTs by β-cyclodextrin results in the stable CNT fluid, which enhances the solar absorptivity and thermal conductivity [126]. Similar properties can be achieved by synthesizing partially unzipped multi walled carbon nanotubes (PUMWCNTs) via modified Hammers method, which gives 1D MWCNTs and 2D graphene nanoribbon hybrids having no agglomeration [123].

Photovoltaic cells (PVCs) based on carbon have attracted scientists' interest. CNTs are considered to be p-type semiconductors, with an extraordinary mobility [127]. The combination of CNTs with electron donors shows that a new idea to utilize solar energy, and to transform it into electrical

energy [128]. The introduction of CNTs such as C_{60} into the conjugated polymers is used for the production of organic photovoltaic devices [129]. Recently, double-walled CNT (DWCNT)/n-Si heterojunction-based solar cells have been designed, because of the extremely conductive and transparent nature of DWCNT films [130,131]. Apart from silicon, the heterojunction of CNTs with n-type gallium arsenide (n-GaAs) have also been developed [132]. The resulting efficiency is up to 3.8%, with the illumination of a green laser or desk lamp. The above outcomes indicate that carbon-on-Si is a considerable pattern for producing solar cells with outstanding conversion efficiency.

CNTs also play a vital role in ultracapacitors or electrochemical double-layer capacitors (EDLCs), which are devices for energy storage based on the principle of the double layer effect [133]. The ultracapacitors with electrodes, composed of CNTs with vertical alignment has an enhanced power density of almost four times greater than batteries, a lifespan more than 300,000 cycles, and an energy density of approximately 60 W/kg [103]. The substantial improvement in the DLC power density arises from the extraordinary conductivity, and surface area obtained from CNTs [109].

Owing to their promising electrochemical properties, CNTs have been getting remarkable consideration as a candidate electrode material for batteries. The synthesis of SnO–CNT composites provides excellent anode material for the technologically appreciated lithium ion batteries (LIBs) [134]. The fabrication of high-performance electrodes for LIBs can be designed by the combination of CNTs with Si nanoparticles [135,136]. The best flexible anode structure, comprising of Si-coated CNTs requires some structural features, i.e., (a) no binder; (b) no current collector; (c) flat film with low density; (d) CNTs with appropriate porosity for uniform silicon coating; and (e) an aligned CNT structure to cushion the volumetric expansion of Si during cycling. These problems have directed the scientists towards the fabrication of different electrode structures.

Figure 11 indicates that silicon (Si) electrode shows poor cycling performance after 40 cycles (100 mAh g^{-1}) (first cycle reversible capacity of 2780 mAh g^{-1}). The carbon coated Si (Si@C) reveals significantly enhanced cycling stability. This stability is due to the homogenous layer of carbon on the Si nanoparticles that controls the volumetric changes and enhances the conductivity, resulting in capacity retention of 48% after 40 cycles. For carbon-coated Si-CNT composite (Si@C-CNTs), a slight improvement of reversible capacity is detected during the first five cycles and subsequently began declining. Among all of the three anodes, the Si@C–CNTs anode demonstrates the highest cycling stability, with a 70% capacity retention after 40 cycles [137].

CNTs have gained recent attention for their use in microbial fuel cells (MFC), due to their excellent and unique intrinsic properties, such as corrosion resistance, good electrochemical stability, and high conductivity [138].

We can consider a MFC as a bioelectrochemical device that convert biomass into electricity and harvests electricity generated by the oxidation of the substrate during the anaerobic respiration of a particular bacterial species. The anaerobic respiration and oxidation of substrate takes place in the anodic chamber. Therefore, the type of anode material is very important in determining the efficiency and power output of MFC. An increasing preference has been seen in using CNTs for the reduction in the external resistance of MFCs. The CNTs are considered as beneficial for increasing the efficiency of nutrient–proton–oxygen transfer through the biofilm. Moreover, the CNT-based anodes are reported to lower cellular toxicity and kinetic losses [139]. Ren et al. [140] analyzed three different CNT-based electrode materials, called randomly aligned (raCNT), vertically aligned (vaCNT), and spin-spray layer-by-layer (SSLBL) CNTs. CNT materials with a surface area-to-volume ratio of about 4000 m^{-1} are preferred. It was demonstrated that, in comparison with bare gold, CNT-based materials were able to attract more exoelectrogens and *Geobacter* species. This consequently leads to the formation of a denser biofilm with an extreme power production density of 3320 W m^{-3}, which is 8.5 times higher than attained using 2D-electrode systems. Moreover, carbon nanotube-textile (CNT-textile) has also been used for the growth of MFCs, with enhanced activity [138,141,142]. This biocompatible CNT-textile is highly conductive, and its 3D structure helps in the formation of a biofilm that is 10 times thicker than with an unmodified textile. It also eases the transport of the substrate to the biofilm, and an interior

settlement of a different groups of microbial community. It has been reported that the CNT–textile anode has 10 times less charge transfer resistance (Rct), and 157% higher current density. A 141% energy recovery and 68% power density were also achieved [143].

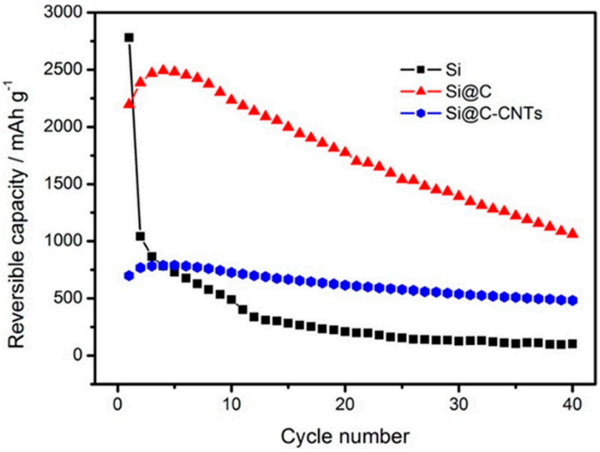

Figure 11. Cycling performance of Si, Si@C, and Si@C–CNTs at 100 mA g^{-1} in a 0.02–2.0 V voltage window. Reproduced with permission from [137]. Copyright ACS, 2012.

Indeed, the CNT-textiles anode was proven to be appropriate for enhancing the activity of MFC. The coating of CNT on macroporous sponge gives rise to an improved version of the CNT-textile [144]. This CNT-sponge exhibited improved stability, low internal resistance, and a well-ordered 3D CNT surface with a flexible structure and enhanced mechanical strength. The achievable current density was up to 48% higher compared to that achieved with CNT-textile under similar environments [142,143]. CNT, when used as the anode material, enhanced the power production of the MFC, and showed tolerance to high concentration of substrate.

He et al. reported the use of CNTs as an anode material to design a novel up-stream fixed-bed microbial fuel cell (FBMFC). The interest in the fabrication of FBMFC was the achievement of effective wastewater handling ability with good power generation. Around 90% of the chemical oxygen demand (COD) removal was accomplished by the reactor [144]. It has been investigated that the composite electrode based on carbon nanofiber improved graphite fibers (CNFs/GF) enhances the activity of MFC by approximately seven times, as compared to unmodified graphite fibers [145]. Similarly, the use of an ultra-thin activated carbon nanofiber nonwoven (ACNFE) porous structure with a large surface area offered a greater area for the coverage of the biofilm, for improved activity via reducing the limitation of mass transfer [146]. Figure 12 shows SEM micrographs of some composite anode materials.

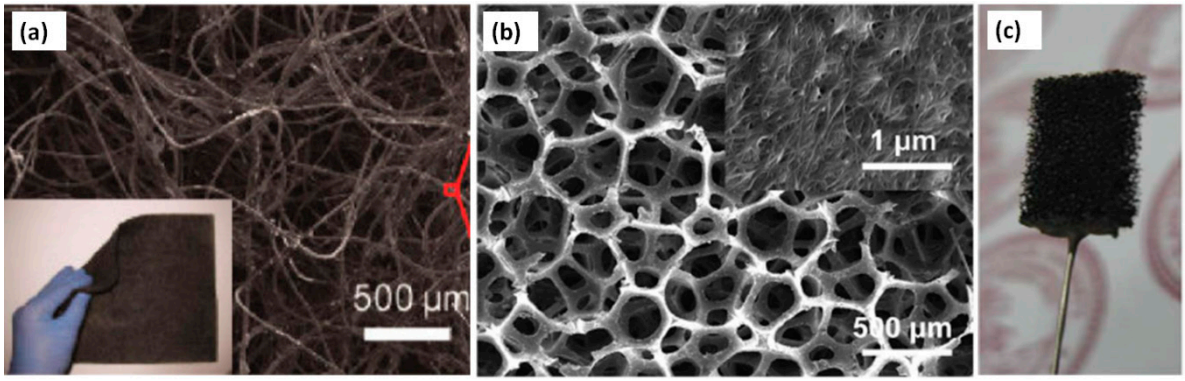

Figure 12. SEM micrographs of composite anode materials (**a**) CNT-textile (**b**) CNT-sponge (**c**) Picture of a CNT-sponge electrode. Image (a): Reproduced with permission from [142]. Copyright ACS, 2011. Image (b) and (c): Reproduced with permission from [143]. Copyright RSC, 2012.

5.2. Water Treatment

CNTs, as compared to activated carbon, have a high ratio of surface active sites to volume, and an organized distribution of pore size, due to which they have excellent sorption ability. The nature of the sorbate and the functional groups on the surface also influence the adsorption capacity of CNTs. All living organisms need clean water to nourish life. Different heavy metals can be removed from water by using CNTs as adsorbents, and they can be used extensively for water treatment applications. Mercury is a non-essential trace metal, and it is very toxic to all living organisms. CNT-based ultrasensitive sensors are used for the detection of mercury in water [147]. It can be removed by adsorption, using COO^- functionalized CNTs [148]. Similarly, the use of CNTs with two different morphologies in mullite pore channels act as a unique adsorptive membrane for the removal of nickel ions from water [149].

Moreover, functionalized CNTs have the capability to absorb Mn(VII) on their surface from water, by dispersing in it for a little time [150]. Table 2 shows heavy metal adsorption onto various types of CNTs.

Table 2. Adsorption of heavy metal ions onto different types of CNTs.

Adsorbents	Metal Ions	Adsorption Capacity (mg g^{-1})	Reference
CNTs	Pb^{2+}	17.44 (pH 7.0)	[151]
CNTs (HNO_3)	Pb^{2+}	49.95 (pH 7.0)	[152]
MWCNTs	Ni^{2+}	7.53 (pH 7.0)	[153]
MWCNTs (HNO_3)	Pb^{2+}	97.08 (pH 5.0)	[154]
CNT–OH	Cu^{2+}	1.342	[148]
CNT–COO^-	Cd^{2+}	3.325	[148]
CNT–CONH	Hg^{2+}	1.658	[148]
CNT–COO^-	Hg^{2+}	3.300	[148]

Besides the removal of toxic metals, CNTs also play a vital role in the removal of various organic pollutants, in the process of water treatment. Many organic dyes, even in low concentration in water, are very toxic and carcinogenic in nature. Research interest is focused on using different adsorbents for treating organic dyes before introducing them into the environment. Due to the large surface area and extraordinary properties of CNTs, they are considered an excellent adsorbent for the treatment of organic dyes [155]. Wu evaluated the CNTs performance for Procion Red MX-5B dye adsorption, present in different industrial wastes [156]. Similarly, COOH-functionalized MWCNTs have great adsorption ability, which is mostly based on high surface area, adequate pore structure, and the existence of a broad spectrum of surface functional groups. These numerous chemical sorption sites on functionalized CNTs improve the attraction for metal ions, and also for dyes [157].

Furthermore, the nanostructured material synthesized by MWCNTs-supported palladium (Pd) nanocubes is used to remove methyl orange (MO) [158]. The nanocubes can be synthesized in two ways (i) by reducing H_2PdC_{14} (ii) by a non-covalent method that involves the use of a surfactant for carbon nanotubes functionalization. The performance of MWCNTs/Pd nanomaterial is estimated by the discoloration of a MO aqueous solution at various intervals of time. Figure 13 shows the UV-vis spectra of MO, with a peak of maximum absorption at 463 nm, which is slowly decreasing, and finally nearly disappears, showing the removal of MO. MWCNTs result in decontamination, by adsorbing organic dyes on its surface, which can be catalyzed by Pd nanocubes, by which the MWCNTs/Pd-based nanostructured material has enhanced decontamination efficiency instead of untreated MWCNTs. However, Pd nanocubes alone neither adsorb nor decompose the contaminants, to enhance decontamination efficiency [158]. Some other organic toxins other than dyes, are drugs, phenols, aromatic amines, insecticides, and other poisonous organics. They have shown adverse effects on the environment, mostly onto the water sources. Many research groups have used CNTs to remove

various organic toxins from water, and have investigated their performances, which is summarized in Table 3.

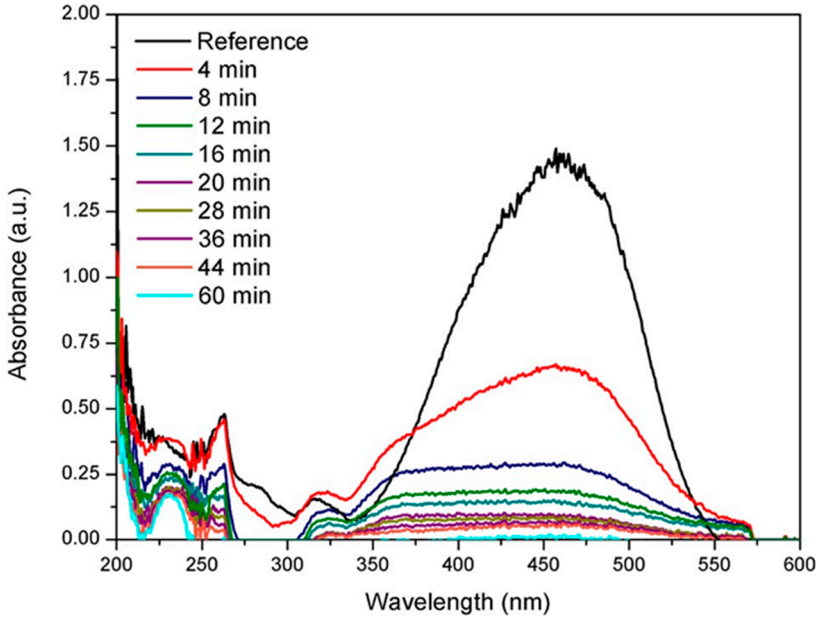

Figure 13. UV-vis spectra showing methyl orange degradation using MWCNTs/Pd nanostructured material. Reproduced with permission from [158]. Copyright Elsevier, 2016.

Table 3. Removal of organic toxins via different types of CNTs.

Type of CNTs	Organic Pollutants	Adsorption Capacity (mg g^{-1})	Reference
Alkali-activated MWCNTs	Methylene blue	399	[159]
Untreated MWCNTs	Methylene blue	59.7	[160]
Untreated SWCNTs	Dissolved organic matter (DOM)	26.1–20.8	[161]
Calcium alginate/MWCNTs	Methyl orange	12.5	[162]
Carboxylated multiwalled carbon nanotubes	Norfloxacin	90.3	[163]
Single-, double-, and multiwalled carbon nanotubes	Ciprofloxacin	933.8, 901.2, 651.4	[164]
Pristine and hydroxylated MWCNTs	Sulfamethazine	24.78, 13.31	[165]

CNTs also play a key role in the removal of oil from water. This is an extremely significant area because of the enormous manufacturing rate of emulsified oil in water, which is one of the main toxins having a negative impact on the environment and on living organisms. High-quality CNT bundles synthesized by an injected vertical chemical vapor deposition (IV-CVD) reactor are used for the separation of oil. Two kinds of CNTs are used for oil separation from water; namely, produced CNTs (P-CNTs) and commercial CNTs (C-CNTs). An enhanced removal efficiency of approximately 97% is attained by using P–CNTs, as compared to 87% when using C–CNTs [166]. Figure 14 shows the effect of contact time on the percentage removal of oil, and the change in oil concentration in water with respect to time.

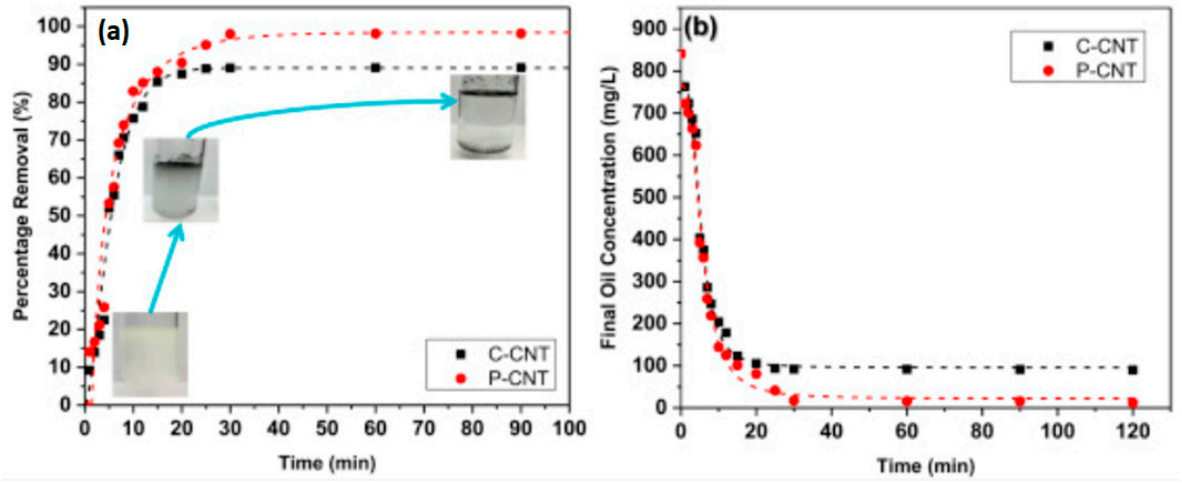

Figure 14. (**a**) The effect of interaction time and the % removal of oil, along with the digital image (**b**) change in oil concentration in water as function of time. Reproduced with permission from [166]. Copyright Elsevier, 2016.

5.3. Biomedical Applications

Applications of nanotubes cover various fields such as nanotechnology, medication, industrialization, electronics, and so on. There are some barriers such as the functionalization, toxicity, and pharmacology of CNTs, which must be overcome before using CNTs in biological and biomedical environments [25]. Sensors fabrication is one of the most significant applications of functionalized CNTs. The DNA sequences in the body can be detected by CNT-based nanobiosensors [167]. CNT-based pressure sensors can be used in eye surgeries, kidney dialysis machines, respiratory devices, and hospital beds [168,169]. Furthermore, MWCNTs modified by nitric acid-sulfuric acid treatment dispersed in polyvinylpyrrolidone (PVP) are used for the preparation of electroconductive electrodes on polyvinylidene fluoride (PVDF) filters for sensing and taping electrocardiograms [170]. A literature study indicates that CNTs can function as actuators, and that these CNT-based actuators can perform at low voltages and high temperatures up to 350 °C, and in a physiological environment [171,172]. The polymer composites based on CNTs, due to their strength, stiffness, and relatively low operating voltage, can be used as artificial muscle devices [173]. There is an expansion and contraction in the CNT mats when they are operated in an electrochemical cell as assembled electrodes. By applying the electric potential, the charging of electrodes occurs, and due to the introduction of the electronic charge, the length of the CNT changes linearly. This linear change in the length is due to the charge rearrangement in the double layer outside the tube [174]. CNTs play a major role in the identification of cancer cells [175]. As cancer is asymptomatic in its early stages, therefore, imaging methods, such as magnetic resonance imaging (MRI), cross-sectional tomographic image (CT) and X-ray do not obtain spatial determination for early-stage recognition of the disease [25]. However, good tissue penetration can be attained when functionalized SWCNTs are applied to MRI [176]. The use of CNTs can also be extended to implantation technology, such as artificial joints and many other implants. Usually, the body faces certain complications to implants, along with post-administration pain. However, tiny nanotubes and nanohorns interfere with some amino acids and proteins and make implants acceptable to the body [177]. Because of the CNTs' extraordinary tensile strength, they can function as an alternative to bone, and when packed with calcium, and organized into the bone structure, can act as [178,179]. Table 4 shows some of artificial implants. In cancer cells, the overexpression of certain protein biomarkers often provide a clue to initial diagnosis, examining remedies for advanced disease, maintaining scrutiny following medicinal surgery, and predicting therapeutic reactions [25]. Table 5 shows the summary of the detection of cancer biomarkers by detection systems based on CNTs. Due to the ultrahigh surface area of CNTs, and their needle-like structures, they find applications in drug delivery and genetics, and are excellent materials for the delivery of nucleic acids, drugs,

and peptides. CNTs are commonly used for carrying molecules of therapeutic importance through biological membranes, and thus, they have widely been investigated for applications in the field of theranostics [180]. By nature, CNTs act as antioxidants, and they are used to shield drug preparations that are considered prone to oxidation. Due to their antioxidant character, they are used in cosmetics for delayed aging, and as suntan lotion to avoid sunburn and skin carcinoma by preventing the oxidation of the main constituents of skin [177].

Table 4. Applications of CNTs as artificial implants.

Type of CNT	Materials Type	Type of Cell or Tissue	Properties	Reference
Porous SWCNT	Polycarbonate membrane	Osteoblast-like cells	Enhances lamellipoda (cytoskeletal) extensions, and lamellipodia extensions	[181]
SWCNT-incorporated	Chitosan scaffolds	C_2C_{12} cells/C_2 myogenic cell line	Improvement in cell growth	[182]
MWCNT	Collagen sponge honeycomb scaffold	MC_3T_3-E_1 cells, a mouse osteoblast-like cell line	Enhances proliferation and cellular adhesion	[183]
MWCNT	Polyurethane	Fibroblast cells	Improve cellular interactions and the polyurethane surface	[184]
MWCNT	Alginate	Rat heart endothelial cell	Improvement in cellular adhesion and proliferation	[185]
MWCNT	Poly(acrylic acid)	Human embryonic stem cells	Increase cellular differentiation toward neurons	[186]
SWCNT	Propylene fumarate	Rabbit tibia	Support the attachment of cells and proliferation	[187]

Table 5. Examples of detection of cancer biomarkers by CNTs.

Carbon nanotube	Biomarker	Form of Cancer	Reference
Multilabel secondary antibody-nanotube bioconjugates	Prostate-specific antigen (PSA)	prostate cancer	[188]
Microelectrode arrays modified with single-walled carbon nanotubes (SWNTs)	Total prostate-specific antigen (T-PSA)	Prostate cancer	[188]
Multiwalled carbon nanotubes–thionine–chitosan (MWCNTs–THI–CHIT) nanocomposite film	Chlorpyrifos residues	Many forms	[189]
Tris(2,2′-bipyridyl)cobalt(III) (Co(bpy)33+)–MWNTs–Nafion composite film	Carcinoma antigen-125 (CA125)	Carcinoma	[190]
Carbon nanotube field effect transistor (CNT-FET)	Prostate-specific antigen (PSA)	Prostate cancer	[191]
Multiple enzyme layers assembled multiwall carbon nanotubes (MWCNTs)	Alpha-fetoprotein (AFP)	Many forms	[192]

5.4. Electronic Applications

CNTs have the potential to be used in the field of electronics. Now, scientists are capable of the enormously enhanced integration density of the device, thus attaining enhanced speed and efficiency with promising applications in energy saving and integrated circuits. It is understood that CNT-electronics share the potential, together with biotechnology, for the advancement of current devices [3]. Some of their applications are given below.

5.4.1. Carbon Nanotube-Based Diodes, Field-Effect Transistors, and Logic Circuits

CNTs (SWNTs) can form perfect p–n junction diodes owing to their excellent mechanical and electrical properties [193]. The use of CNTs instead of conventional transistors and diodes significantly increases the current-carrying capability of the devices, while reducing the operational temperature. SWNT diodes exhibit excellent power conversion efficiencies when illuminated, due to improved diode

properties [194]. Non-covalent doping can tune the doping type and degree of the SWNT without producing structure defects [195]. The diameter of SWCNT can be used to control its energy gap to produce the p-n junction diodes with different characteristics [196]. Furthermore, the characteristics of high intrinsic mobility (>100,000 cm^2/Vs) and up to 109 A cm^{-2} current-carrying capacity make SWNTs promising for use in the high-performance diodes fabrication [197]. CNTs with a semiconducting nature show the required properties for producing field-effect transistors and logic switches. The mutual properties of both metallic and semiconducting types of CNTs can form special building blocks for future electronics [198]. The key components of a classic FET which is a three terminal device are the source (S), drain (D) and gate (G) electrodes; a channel between the source and drain; and a dielectric (typically oxide) that separates the gate from the channel. FET via the gate voltage VG mainly controls the device resistance or drain-source current (IDS) in the channel, and also amplify signals. The two key parameters characterize the FET-switching behavior. One reflects the FET-magnifying ability which is the transconductance, while the second one is sub-threshold swing (SS) that calculates the FET speed at which it can be switched to an on-current or on-state from an off-current or off-state. In general, the FET is faster for the smaller SS [199]. SWCNT field-effect transistors (FETs) have some important properties as compared to conventional semiconductor transistors, which make them unique and interesting: (i) the one-dimensional CNT decreases the possibility of scattering [200]. As a result, the devices may function with extreme speed; (ii) the conduction usually occurs on its surface where the bonds are saturated and stable. Therefore, there is no interface passivation required in between the gate dielectric and the nanotube channel; (iii) In an intrinsic nanotube device, the Schottky barrier at the metal–nanotube contact is the active switching element [201]. As an alternative to conventional CMOS (complementary metal oxide semiconductor)-based logic gates, carbon nanotube field-effect transistors (CNFETs) in a circuit can do simple logic functions, and this results in lower power consumption and greater stability, favoring greater gain, and allowing for easy application in integrated circuits [103,198].

5.4.2. CNT-Based Sensors

Sensors continue to have a significant impact in everyday life. Nowadays, research has been focused on producing extremely sensitive, responsive, selective, and cost-effective sensors for various applications. Carbon-based nanomaterials, especially CNTs, have a lot of different properties that can be taken into consideration for designing advanced sensors, capable of decreasing the power consumption, and reducing the weight and cost [202]. CNT-based biosensors exhibit great advantages over the commercially available metal oxide- and silicon-based biosensors. Owing to their enhanced surface-to-volume ratio and hollow pipe, CNT-based biosensors exhibit high sensitivities and fast response times, and they can be used for enzyme immobilization [203], which possess enhanced biological activity. CNTs can promote reactions involving electron transfer, similar to NADH and hydrogen peroxide [204]. These biosensors have lower potentials for redox reactions, lower surface fouling effects, high stabilities, and longer life times. For ultra-sensitive biosensing systems, these properties make CNT-based biosensors the next generation of building blocks [204]. Zhigang Zhu et al. detected glucose solution using CNT fiber-based sensing electrodes [205]. Furthermore, Fatoni and his co-workers synthesized a chitosan–bovine serum albumin (Chi–BSA) cryogel-based stable glucose biosensor with incorporated MWCNTs, GOD, and ferrocene (Fc) [206]. Besides, Xianwen Kan et al. fabricated MIPs/MWNTs/GCE-based molecularly imprinted polymers glassy carbon electrodes for the recognition and determination of dopamine [207]. In addition, the contact of CNTs or CNTs-based composites with certain gases causes changes in their properties, and can be identified by different techniques. As a result, theoretical evaluations of gas adsorption and gas-sensing systems based on CNTs have been the topics of extensive research [202,208]. Hu Young Jeong et al. synthesized polyimide-supported vertical carbon nanotubes (CNTs)/reduced graphene hybrid film-based NO_2 gas sensors that can work at room temperature [209]. Sukhananazerin and his co-workers prepared nanocomposite of polyaniline-functionalized multiwalled carbon nanotubes (PANI/MWCNTs), and employed it as gas sensor that showed excellent ammonia (NH_3) gas detection at a trace level [210].

5.4.3. Field Emission

CNTs, due their high chemical stability, a sharp tip, better mechanical power, and good aspect ratio, are appropriate to be used as field emission electron sources [211] for flat panel displays [212,213], lamps [211], gas discharge tubes providing surge protection [214], and X-rays [215]. CNT emitters, as compared to thermoionic ones, act as better energy savers and show steady operation, as no preheating is required for the emission of electrons from the cathode surface [211]. Nanotubes are well researched for their outstanding electron sources at very low fields, producing a very steady current, and they have the ability to function at adequate vacuum. In comparison to silicon-grown CNTs, metallic substrates like copper-grown CNTs result in decreased contact resistance. The combination of CNTs and the metallic substrate ensure easy electron transport, while the emitters during the process of emission withstand high currents, owing to the rigidity of these nanostructures [216]. Methods have been established to shape the films, and change the nanotubes density and their arrangement on the substrate, so as to enhance their emission properties [103]. By the neighboring CNTs, a high-density array of CNTs in electric field screening therefore reduces the emission current, whereas poor emission from a low density of CNTs is due to the smaller number of emission sites availability. Catalyst patterning has achieved selected area low-density growth of CNTs, using nanosphere lithography (NSL) [217] electron beam lithography [218], photolithography [219], focused ion beam lithography [220], and chemical etching [221]. Dionne et al. have investigated individual as well as arrays of CNTs field enhancement factors [222].

5.4.4. Transparent Electrodes

Transparent conductive electrodes (TCEs), which simultaneously conduct the current and transmit light mostly in the visible spectral range, are of great significance. These materials have been identified since the end of the 19th century, the first example being the thin metal films that are synthesized by sputtering and evaporation [223]. Badeker was the first scientist to examine transparent conductive oxide (TCOs) such as CdO [224]. Optically transparent electrodes (OTEs) are important constituents of organic-based solar cells, as well as light-emitting diodes (OLEDs). CNT-based thin sheets are investigated as valid substituents for indium tin oxide (ITO) transparent conductors, owing to their extra flexible nature, and they have the potential to be used in touch screens and flexible displays as a highly transparent, conductive, and cost-effective alternative [225].

5.4.5. CNTs as Probes in Atomic Force Microscopy

Measuring the conductive properties of surfaces using atomic force microscope (AFM) techniques has been in use for 20 years [226]. Conductive AFM (C-AFM) has been used to characterize the electrical properties of conducting and semi-conducting samples, whilst simultaneously collecting surface topography [227]. The conducting AFM tip is a crucial component of C-AFM, and it is the key factor in determining the quality and resolution of the data acquired. The technology for the fabrication of AFM probe tips is undergoing rapid evolution with the application of new nanotechnology techniques [228]. There are many different types of commercially available conducting AFM probes. Low-cost C-AFM tips consist of a standard silicon cantilever coated with a 20–40 nm thick metal film. The metals used include single elements like gold, or they may consist of an alloy such as platinum/iridium [229]. Unlike standard silicon AFM probes, CNTs are not brittle, and they do not wear easily. CNTs are capable of transmitting proportionately large forces given their nanoscale dimensions. Under large compression forces, CNTs will bend without breaking, and when the applied force is removed, the CNT will recover its original conformation with little or no plastic deformation [228]. Due to the stiffness and wear resistance of CNTs, they are considered to be an ideal imaging tip for atomic force microscopy (AFM) applications [12,230].

5.5. Buckypaper

CNT buckypapers are tangled assemblies of CNT films with 2D paper-like ropes cohesively bounded via Van der Waals interactions [231]. Macroscopic buckypapers can reveal uncanny multi-functionalities in aggregation with mechanical stability [232], flexibility [233], high electrochemical activity, and thermal and electrical conductivities [234]. Buckypapers have little contact resistance and a significantly higher conductivity than the traditional macroscopic CNT materials like CNT composites, owing to their continuous nanotube networks [235]. Due to their open cellular structure, buckypapers possess highly accessible surface areas, resulting in high electrochemical activity per unit mass of electrode [236]. Besides, the substantial mechanical strength of the CNT networks permits the realization of flexible yet robust devices. Consequently, this material is used in diverse applications such as artificial muscles [237], drug delivery [238], electrodes [239], AFM probes [229] field-emission [240], fire shields [241], and for water purification [242]. Several techniques have been used to fabricate buckypapers, such as the vacuum filtration method [243], the chemical vapor deposition method [244], spin-coating techniques [245], and the Langmuir–Blodgett assembly method [246].

6. Conclusions

Carbon nanotubes have the potential to be explored further, and the progress made in the use of CNTs in various fields can be pushed farther. The results achieved in the synthesis, functionalization, and design of CNTs have greatly contributed to promising advancements in different areas. However, further improvements in the synthesis methods are required to obtain CNTs for the desired applications. For example, the catalyst size influences the CNT diameter as synthesized by CVD. Hence, further work could be done in order to find more efficient ways to prepare exactly uniform-sized catalyst particles, so that production of a particular diameter of SWCNTs can be attained. In addition, the cost of CNTs is high, as compared to other nano-carbon materials. Attempts should be made to search for new sources of carbon that are cost-effective and abundant, so that the price of CNTs can be decreased to an appropriate level.

The constant miniaturization of electronic devices is the most energetic force of the microelectronic industry. All over the world, the aim of scientists is to manufacture tiny devices with sizes comparable to those of molecules or bunches of atoms. The utilization of the unusual properties of SWCNTs could lead to electronic devices having nanometer-range sizes. Such a highly productive potential and applications has forced scientists to investigate certain techniques to use them. One day, CNTs will replace metal filaments in X-ray machines, which used to burn out quickly. This may improve portable X-ray machines that can be used in ambulances, customs work, and airport security. There is no doubt that CNTs in the near future will become indispensable not only commercially, but they will also particularly will find applications in energy storage and conversion.

The constant miniaturization of electronic devices is the most energetic force of the microelectronic industry. All over the world, the aim of researchers is to manufacture tiny devices of molecules or bunch of atomic size. The utilization of the unusual properties of SWCNTs could lead to electronic devices in the nanometer range. Such a highly productive potential and applications have forced scientists to investigate certain techniques to use them. One day CNTs will replace metal filaments in the X-ray machines, which are used to burn out quickly. This may improve portable X-ray machines that can be used in ambulances, customs work, and airport security. There is no doubt that CNTs in the near-future will become indispensable, not only commercially, but particularly will find applications in energy storage and conversion.

Author Contributions: Z.N. performed literature survey under the supervision of G.R. A.u.H.A.S. and S.B. All the authors collaborated in manuscript writing.

Funding: This research received no external funding.

Acknowledgments: The authors are thankful to all the members of Materials Chemistry Lab, Institute of Chemical Sciences, University of Peshawar, Pakistan for their support and fruitful discussion.

Conflicts of Interest: The authors declare no conflict of interest.

References

1. Coville, N.J.; Mhlanga, S.D.; Nxumalo, E.N.; Shaikjee, A. A review of shaped carbon nanomaterials. *S. Afr. J. Sci.* **2011**, *107*, 1–15. [CrossRef]
2. Rius, G. Technologies of Carbon Materials. Syntheses and Preparations. In *Carbon for Sensing Devices*; Springer: Cham, Switzerland, 2015; pp. 15–42.
3. Lee, J.; Kim, T.; Jung, Y.; Jung, K.; Park, J.; Lee, D.-M.; Jeong, H.S.; Hwang, J.Y.; Park, C.R.; Lee, K.-H. High-strength carbon nanotube/carbon composite fibers via chemical vapor infiltration. *Nanoscale* **2016**, *8*, 18972–18979. [CrossRef] [PubMed]
4. Chua, M.; Chui, C.-K.; Chng, C.-B.; Lau, D. Carbon nanotube-based artificial tracheal prosthesis: Carbon nanocomposite implants for patient-specific ENT care. *IEEE Nanotechnol. Mag.* **2013**, *7*, 27–31. [CrossRef]
5. Ketabi, S.; Rahmani, L. Carbon nanotube as a carrier in drug delivery system for carnosine dipeptide: A computer simulation study. *Mater. Sci. Eng. C* **2017**, *73*, 173–181. [CrossRef] [PubMed]
6. Arunachalam, S.; Gupta, A.A.; Izquierdo, R.; Nabki, F. Suspended Carbon Nanotubes for Humidity Sensing. *Sensors* **2018**, *18*, 1655. [CrossRef] [PubMed]
7. Kumar, S.; Nehra, M.; Kedia, D.; Dilbaghi, N.; Tankeshwar, K.; Kim, K.-H. Carbon nanotubes: A potential material for energy conversion and storage. *Prog. Energy Combust. Sci.* **2018**, *64*, 219–253. [CrossRef]
8. Puett, C.; Inscoe, C.; Hartman, A.; Calliste, J.; Franceschi, D.K.; Lu, J.; Zhou, O.; Lee, Y.Z. An update on carbon nanotube-enabled X-ray sources for biomedical imaging. *Wiley Interdiscip. Rev. Nanomed. Nanobiotechnol.* **2018**, *10*, e1475. [CrossRef]
9. Sun, Y.; Yun, K.N.; Leti, G.; Lee, S.H.; Song, Y.-H.; Lee, C.J. High-performance field emission of carbon nanotube paste emitters fabricated using graphite nanopowder filler. *Nanotechnology* **2017**, *28*, 065201. [CrossRef]
10. Zhao, T.; Ji, X.; Jin, W.; Yang, W.; Li, T. Hydrogen storage capacity of single-walled carbon nanotube prepared by a modified arc discharge. *Fuller. Nanotubes Carbon Nanostruct.* **2017**, *25*, 355–358. [CrossRef]
11. Xu, J.-L.; Dai, R.-X.; Xin, Y.; Sun, Y.-L.; Li, X.; Yu, Y.-X.; Xiang, L.; Xie, D.; Wang, S.-D.; Ren, T.-L. Efficient and reversible electron doping of semiconductor-enriched single-walled carbon nanotubes by using decamethylcobaltocene. *Sci. Rep.* **2017**, *7*, 6751. [CrossRef]
12. Choi, J.; Park, B.C.; Ahn, S.J.; Kim, D.-H.; Lyou, J.; Dixson, R.G.; Orji, N.G.; Fu, J.; Vorburger, T.V. Evaluation of carbon nanotube probes in critical dimension atomic force microscopes. *J. Micro/Nanolithogr. MEMS MOEMS* **2016**, *15*, 034005. [CrossRef] [PubMed]
13. Chen, S.; Shan, B.; Yang, Y.; Yuan, G.; Huang, S.; Lu, X.; Zhang, Y.; Fu, Y.; Ye, L.; Liu, J. An overview of carbon nanotubes based interconnects for microelectronic packaging. In Proceedings of the 2017 IMAPS Nordic Conference on Microelectronics Packaging (NordPac), Gothenburg, Sweden, 18–20 June 2017; pp. 113–119.
14. Lukyanovich, V. The structure of carbon forming in thermal decomposition of carbon monoxide on an iron catalyst. *Sov. J. Phys. Chem.* **1952**, *26*, 88–95.
15. Oberlin, A.; Endo, M.; Koyama, T. Filamentous growth of carbon through benzene decomposition. *J. Cryst. Growth* **1976**, *32*, 335–349. [CrossRef]
16. Iijima, S. Helical microtubules of graphitic carbon. *Nature* **1991**, *354*, 56–58. [CrossRef]
17. Dresselhaus, M.; Dresselhaus, G.; Saito, R. Physics of carbon nanotubes. *Carbon* **1995**, *33*, 883–891. [CrossRef]
18. Saito, R.; Dresselhaus, G.; Dresselhaus, M.S. *Physical Properties of Carbon Nanotubes*; World Scientific: Singapore, 1998; Vol. 35.
19. Zhang, F.; Hou, P.-X.; Liu, C.; Cheng, H.-M. Epitaxial growth of single-wall carbon nanotubes. *Carbon* **2016**, *102*, 181–197. [CrossRef]
20. Ding, R.; Lu, G.; Yan, Z.; Wilson, M. Recent advances in the preparation and utilization of carbon nanotubes for hydrogen storage. *J. Nanosci. Nanotechnol.* **2001**, *1*, 7–29. [CrossRef]
21. Tang, Z.; Zhang, L.; Wang, N.; Zhang, X.; Wen, G.; Li, G.; Wang, J.; Chan, C.; Sheng, P. Superconductivity in 4 angstrom single-walled carbon nanotubes. *Science* **2001**, *292*, 2462–2465. [CrossRef]
22. Al Moustafa, A.-E.; Mfoumou, E.; Roman, D.E.; Nerguizian, V.; Alazzam, A.; Stiharu, I.; Yasmeen, A. Impact of single-walled carbon nanotubes on the embryo: A brief review. *Int. J. Nanomed.* **2016**, *11*, 349. [CrossRef]
23. Iijima, S.; Ichihashi, T. Single-shell carbon nanotubes of 1-nm diameter. *Nature* **1993**, *363*, 603. [CrossRef]

24. Zhang, L.; Chen, L.; Liu, J.; Fang, X.; Zhang, Z. Effect of morphology of carbon nanomaterials on thermo-physical characteristics, optical properties and photo-thermal conversion performance of nanofluids. *Renew. Energy* **2016**, *99*, 888–897. [CrossRef]
25. Eatemadi, A.; Daraee, H.; Karimkhanloo, H.; Kouhi, M.; Zarghami, N.; Akbarzadeh, A.; Abasi, M.; Hanifehpour, Y.; Joo, S.W. Carbon nanotubes: Properties, synthesis, purification, and medical applications. *Nanoscale Res. Lett.* **2014**, *9*, 393. [CrossRef] [PubMed]
26. Hirlekar, R.; Yamagar, M.; Garse, H.; Vij, M.; Kadam, V. Carbon nanotubes and its applications: A review. *Asian J. Pharm. Clin. Res.* **2009**, *2*, 17–27.
27. Hou, P.-X.; Liu, C.; Cheng, H.-M. Purification of carbon nanotubes. *Carbon* **2008**, *46*, 2003–2025. [CrossRef]
28. Wang, H.; Chhowalla, M.; Sano, N.; Jia, S.; Amaratunga, G. Large-scale synthesis of single-walled carbon nanohorns by submerged arc. *Nanotechnology* **2004**, *15*, 546. [CrossRef]
29. Anazawa, K.; Shimotani, K.; Manabe, C.; Watanabe, H.; Shimizu, M. High-purity carbon nanotubes synthesis method by an arc discharging in magnetic field. *Appl. Phys. Lett.* **2002**, *81*, 739–741. [CrossRef]
30. José-Yacamán, M.; Miki-Yoshida, M.; Rendon, L.; Santiesteban, J. Catalytic growth of carbon microtubules with fullerene structure. *Appl. Phys. Lett.* **1993**, *62*, 202–204. [CrossRef]
31. Thess, A.; Lee, R.; Nikolaev, P.; Dai, H. Crystalline ropes of metallic carbon nanotubes. *Science* **1996**, *273*, 483. [CrossRef]
32. Seo, J.W.; Magrez, A.; Milas, M.; Lee, K.; Lukovac, V.; Forro, L. Catalytically grown carbon nanotubes: From synthesis to toxicity. *J. Phys. D Appl. Phys.* **2007**, *40*, R109. [CrossRef]
33. Li, Y.; Mann, D.; Rolandi, M.; Kim, W.; Ural, A.; Hung, S.; Javey, A.; Cao, J.; Wang, D.; Yenilmez, E. Preferential growth of semiconducting single-walled carbon nanotubes by a plasma enhanced CVD method. *Nano Lett.* **2004**, *4*, 317–321. [CrossRef]
34. Ebbesen, T.; Ajayan, P. Large-scale synthesis of carbon nanotubes. *Nature* **1992**, *358*, 220. [CrossRef]
35. Szabó, A.; Perri, C.; Csató, A.; Giordano, G.; Vuono, D.; Nagy, J.B. Synthesis methods of carbon nanotubes and related materials. *Materials* **2010**, *3*, 3092–3140. [CrossRef]
36. Teo, K.B.; Singh, C.; Chhowalla, M.; Milne, W.I. Catalytic synthesis of carbon nanotubes and nanofibers. *Encycl. Nanosci. Nanotechnol.* **2003**, *10*, 1–22.
37. Paradise, M.; Goswami, T. Carbon nanotubes–production and industrial applications. *Mater. Des.* **2007**, *28*, 1477–1489. [CrossRef]
38. Journet, C.; Bernier, P. Production of carbon nanotubes. *Appl. Phys. A Mater. Sci. Process.* **1998**, *67*, 1–9. [CrossRef]
39. Landi, B.J.; Raffaelle, R.P.; Castro, S.L.; Bailey, S.G. Single-wall carbon nanotube–polymer solar cells. *Prog. Photovolt. Res. Appl.* **2005**, *13*, 165–172. [CrossRef]
40. Terrones-Maldonado, M. Production and Characterisation of Novel Fullerene-Related Materials: Nanotubes, Nanofibres and Giant Fullerenes. Ph.D. Thesis, University of Sussex, Brighton, UK, 1997.
41. Pandey, P.; Dahiya, M. Carbon nanotubes: Types, methods of preparation and applications. *IJPSR* **2016**, *1*, 15–21.
42. Yang, Q.H.; Bai, S.; Sauvajol, J.L.; Bai, J.B. Large-diameter single-walled carbon nanotubes synthesized by chemical vapor deposition. *Adv. Mater.* **2003**, *15*, 792–795. [CrossRef]
43. Zhang, B.; Chen, Q.; Tang, H.; Xie, Q.; Ma, M.; Tan, L.; Zhang, Y.; Yao, S. Characterization of and biomolecule immobilization on the biocompatible multi-walled carbon nanotubes generated by functionalization with polyamidoamine dendrimers. *Colloids Surf. B Biointerfaces* **2010**, *80*, 18–25. [CrossRef] [PubMed]
44. Couteau, E.; Hernadi, K.; Seo, J.W.; Thien-Nga, L.; Mikó, C.; Gaal, R.; Forro, L. CVD synthesis of high-purity multiwalled carbon nanotubes using $CaCO_3$ catalyst support for large-scale production. *Chem. Phys. Lett.* **2003**, *378*, 9–17. [CrossRef]
45. Ren, Z.; Huang, Z.; Xu, J.; Wang, J.; Bush, P.; Siegal, M.; Provencio, P. Synthesis of large arrays of well-aligned carbon nanotubes on glass. *Science* **1998**, *282*, 1105–1107. [CrossRef] [PubMed]
46. Fan, S.; Chapline, M.G.; Franklin, N.R.; Tombler, T.W.; Cassell, A.M.; Dai, H. Self-oriented regular arrays of carbon nanotubes and their field emission properties. *Science* **1999**, *283*, 512–514. [CrossRef] [PubMed]
47. Patole, S.; Alegaonkar, P.; Lee, H.-C.; Yoo, J.-B. Optimization of water assisted chemical vapor deposition parameters for super growth of carbon nanotubes. *Carbon* **2008**, *46*, 1987–1993. [CrossRef]
48. Chen, J.; Gao, X. Recent Advances in the Flame Synthesis of Carbon Nanotubes. *Am. J. Mater. Synth. Process.* **2017**, *2*, 71. [CrossRef]

49. Merchan-Merchan, W.; Saveliev, A.V.; Kennedy, L.; Jimenez, W.C. Combustion synthesis of carbon nanotubes and related nanostructures. *Prog. Energy Combust. Sci.* **2010**, *36*, 696–727. [CrossRef]
50. Xu, Z.; Zhao, H. Simultaneous measurement of internal and external properties of nanoparticles in flame based on thermophoresis. *Combust. Flame* **2015**, *162*, 2200–2213. [CrossRef]
51. Yuan, L.; Saito, K.; Pan, C.; Williams, F.; Gordon, A. Nanotubes from methane flames. *Chem. Phys. Lett.* **2001**, *340*, 237–241. [CrossRef]
52. Yuan, L.; Saito, K.; Hu, W.; Chen, Z. Ethylene flame synthesis of well-aligned multi-walled carbon nanotubes. *Chem. Phys. Lett.* **2001**, *346*, 23–28. [CrossRef]
53. Lee, G.W.; Jurng, J.; Hwang, J. Formation of Ni-catalyzed multiwalled carbon nanotubes and nanofibers on a substrate using an ethylene inverse diffusion flame. *Combust. Flame* **2004**, *139*, 167–175. [CrossRef]
54. Vander Wal, R.L.; Berger, G.M.; Hall, L.J. Single-walled carbon nanotube synthesis via a multi-stage flame configuration. *J. Phys. Chem. B* **2002**, *106*, 3564–3567. [CrossRef]
55. Vander Wal, R.L.; Ticich, T.M. Flame and furnace synthesis of single-walled and multi-walled carbon nanotubes and nanofibers. *J. Phys. Chem. B* **2001**, *105*, 10249–10256. [CrossRef]
56. Digge, M.; Moon, R.; Gattani, S. Applications of carbon nanotubes in drug delivery: A review. *Int. J. PharmTech Res.* **2012**, *4*, 839–847.
57. Bhaskar, A.; Deshmukh, V.; Prajapati, L. Carbon nanotube as a drug delivery system: A review. *Int. J. Pharm. Technol.* **2013**, *5*, 2695–2711.
58. Annu, A.; Bhattacharya, B.; Singh, P.K.; Shukla, P.K.; Rhee, H.-W. Carbon nanotube using spray pyrolysis: Recent scenario. *J. Alloys Compd.* **2017**, *691*, 970–982. [CrossRef]
59. Yuan, D.; Ding, L.; Chu, H.; Feng, Y.; McNicholas, T.P.; Liu, J. Horizontally aligned single-walled carbon nanotube on quartz from a large variety of metal catalysts. *Nano Lett.* **2008**, *8*, 2576–2579. [CrossRef] [PubMed]
60. Wasel, W.; Kuwana, K.; Reilly, P.T.; Saito, K. Experimental characterization of the role of hydrogen in CVD synthesis of MWCNTs. *Carbon* **2007**, *45*, 833–838. [CrossRef]
61. Jorio, A.; Pimenta, M.; Souza Filho, A.; Saito, R.; Dresselhaus, G.; Dresselhaus, M. Characterizing carbon nanotube samples with resonance Raman scattering. *New J. Phys.* **2003**, *5*, 139. [CrossRef]
62. Dresselhaus, M.; Dresselhaus, G.; Jorio, A.; Souza Filho, A.; Saito, R. Raman spectroscopy on isolated single wall carbon nanotubes. *Carbon* **2002**, *40*, 2043–2061. [CrossRef]
63. Fantini, C.; Jorio, A.; Souza, M.; Ladeira, L.; Souza Filho, A.; Saito, R.; Samsonidze, G.G.; Dresselhaus, G.; Dresselhaus, M.; Pimenta, M. One-dimensional character of combination modes in the resonance Raman scattering of carbon nanotubes. *Phys. Rev. Lett.* **2004**, *93*, 087401. [CrossRef]
64. Jorio, A.; Saito, R.; Hafner, J.; Lieber, C.; Hunter, D.; McClure, T.; Dresselhaus, G.; Dresselhaus, M. Structural (n, m) determination of isolated single-wall carbon nanotubes by resonant Raman scattering. *Phys. Rev. Lett.* **2001**, *86*, 1118. [CrossRef]
65. Milnera, M.; Kürti, J.; Hulman, M.; Kuzmany, H. Periodic resonance excitation and intertube interaction from quasicontinuous distributed helicities in single-wall carbon nanotubes. *Phys. Rev. Lett.* **2000**, *84*, 1324. [CrossRef] [PubMed]
66. Dresselhaus, M.S.; Dresselhaus, G.; Saito, R.; Jorio, A. Raman spectroscopy of carbon nanotubes. *Phys. Rep.* **2005**, *409*, 47–99. [CrossRef]
67. Souza Filho, A.; Jorio, A.; Swan, A.K.; Ünlü, M.; Goldberg, B.; Saito, R.; Hafner, J.; Lieber, C.; Pimenta, M.; Dresselhaus, G. Anomalous two-peak G′-band Raman effect in one isolated single-wall carbon nanotube. *Phys. Rev. B* **2002**, *65*, 085417. [CrossRef]
68. Souza Filho, A.; Jorio, A.; Samsonidze, G.G.; Dresselhaus, G.; Dresselhaus, M.; Swan, A.K.; Ünlü, M.; Goldberg, B.; Saito, R.; Hafner, J. Probing the electronic trigonal warping effect in individual single-wall carbon nanotubes using phonon spectra. *Chem. Phys. Lett.* **2002**, *354*, 62–68. [CrossRef]
69. Wilhelm, H.; Lelaurain, M.; McRae, E.; Humbert, B. Raman spectroscopic studies on well-defined carbonaceous materials of strong two-dimensional character. *J. Appl. Phys.* **1998**, *84*, 6552–6558. [CrossRef]
70. Branca, C.; Frusteri, F.; Magazu, V.; Mangione, A. Characterization of carbon nanotubes by TEM and infrared spectroscopy. *J. Phys. Chem. B* **2004**, *108*, 3469–3473. [CrossRef]
71. Safarova, K.; Dvorak, A.; Kubinek, R.; Vujtek, M.; Rek, A. Usage of AFM, SEM and TEM for the research of carbon nanotubes. *Mod. Res. Educ. Top. Microsc.* **2007**, *2*, 513–519.

72. Oh, S.; Hyon, C.; Sull, S.; Hwang, S.; Park, Y. Detection and volume estimation of semiconductor quantum dots from atomic force microscope images. *Rev. Sci. Instrum.* **2003**, *74*, 4687–4695. [CrossRef]
73. Hata, K.; Futaba, D.N.; Mizuno, K.; Namai, T.; Yumura, M.; Iijima, S. Water-assisted highly efficient synthesis of impurity-free single-walled carbon nanotubes. *Science* **2004**, *306*, 1362–1364. [CrossRef]
74. Huczko, A. Synthesis of aligned carbon nanotubes. *Appl. Phys. A* **2002**, *74*, 617–638. [CrossRef]
75. Kong, J.; Soh, H.T.; Cassell, A.M.; Quate, C.F.; Dai, H. Synthesis of individual single-walled carbon nanotubes on patterned silicon wafers. *Nature* **1998**, *395*, 878–881. [CrossRef]
76. Ural, A.; Li, Y.; Dai, H. Electric-field-aligned growth of single-walled carbon nanotubes on surfaces. *Appl. Phys. Lett.* **2002**, *81*, 3464–3466. [CrossRef]
77. Huang, S.; Cai, X.; Liu, J. Growth of millimeter-long and horizontally aligned single-walled carbon nanotubes on flat substrates. *J. Am. Chem. Soc.* **2003**, *125*, 5636–5637. [CrossRef] [PubMed]
78. Jin, Z.; Chu, H.; Wang, J.; Hong, J.; Tan, W.; Li, Y. Ultralow feeding gas flow guiding growth of large-scale horizontally aligned single-walled carbon nanotube arrays. *Nano Lett.* **2007**, *7*, 2073–2079. [CrossRef] [PubMed]
79. Han, S.; Liu, X.; Zhou, C. Template-free directional growth of single-walled carbon nanotubes on a-and r-plane sapphire. *J. Am. Chem. Soc.* **2005**, *127*, 5294–5295. [CrossRef] [PubMed]
80. Louie, S.G. Electronic properties, junctions, and defects of carbon nanotubes. In *Carbon Nanotubes*; Springer: Berlin/Heidelberg, Germany, 2001; pp. 113–145.
81. Baughman, R.H.; Zakhidov, A.A.; De Heer, W.A. Carbon nanotubes—The route toward applications. *Science* **2002**, *297*, 787–792. [CrossRef] [PubMed]
82. Bachtold, A.; Hadley, P.; Nakanishi, T.; Dekker, C.; Kuzmany, H.; Fink, J.; Mehring, M.; Roth, S. Logic circuits with carbon nanotubes. *AIP Conf. Proc.* **2002**, *633*, 502–507.
83. AuBuchon, J.F.; Chen, L.-H.; Gapin, A.I.; Kim, D.-W.; Daraio, C.; Jin, S. Multiple sharp bendings of carbon nanotubes during growth to produce zigzag morphology. *Nano Lett.* **2004**, *4*, 1781–1784. [CrossRef]
84. Zhang, M.; Li, J. Carbon nanotube in different shapes. *Mater. Today* **2009**, *12*, 12–18. [CrossRef]
85. Iijima, S.; Brabec, C.; Maiti, A.; Bernholc, J. Structural flexibility of carbon nanotubes. *J. Chem. Phys.* **1996**, *104*, 2089–2092. [CrossRef]
86. Yakobson, B.I.; Brabec, C.; Bernholc, J. Nanomechanics of carbon tubes: Instabilities beyond linear response. *Phys. Rev. Lett.* **1996**, *76*, 2511. [CrossRef] [PubMed]
87. Gao, R.; Wang, Z.L.; Fan, S. Kinetically controlled growth of helical and zigzag shapes of carbon nanotubes. *J. Phys. Chem. B* **2000**, *104*, 1227–1234. [CrossRef]
88. Dunlap, B.I. Connecting carbon tubules. *Phys. Rev. B* **1992**, *46*, 1933. [CrossRef]
89. Itoh, S.; Ihara, S. Toroidal forms of graphitic carbon. II. Elongated tori. *Phys. Rev. B* **1993**, *48*, 8323. [CrossRef]
90. Zhang, M.; Nakayama, Y.; Pan, L. Synthesis of carbon tubule nanocoils in high yield using iron-coated indium tin oxide as catalyst. *Jpn. J. Appl. Phys.* **2000**, *39*, L1242. [CrossRef]
91. Hou, H.; Jun, Z.; Weller, F.; Greiner, A. Large-scale synthesis and characterization of helically coiled carbon nanotubes by use of $Fe(CO)_5$ as floating catalyst precursor. *Chem. Mater.* **2003**, *15*, 3170–3175. [CrossRef]
92. Lu, M.; Li, H.-L.; Lau, K.-T. Formation and growth mechanism of dissimilar coiled carbon nanotubes by reduced-pressure catalytic chemical vapor deposition. *J. Phys. Chem. B* **2004**, *108*, 6186–6192. [CrossRef]
93. Wang, J.N.; Su, L.F.; Wu, Z.P. Growth of highly compressed and regular coiled carbon nanotubes by a spray-pyrolysis method. *Cryst. Growth Des.* **2008**, *8*, 1741–1747. [CrossRef]
94. Shaikjee, A.; Coville, N.J. The synthesis, properties and uses of carbon materials with helical morphology. *J. Adv. Res.* **2012**, *3*, 195–223. [CrossRef]
95. Zhou, D.; Seraphin, S. Complex branching phenomena in the growth of carbon nanotubes. *Chem. Phys. Lett.* **1995**, *238*, 286–289. [CrossRef]
96. Scuseria, G.E. Negative curvature and hyperfullerenes. *Chem. Phys. Lett.* **1992**, *195*, 534–536. [CrossRef]
97. Chernozatonskii, L. Carbon nanotube connectors and planar jungle gyms. *Phys. Lett. A* **1992**, *172*, 173–176. [CrossRef]
98. Li, J.; Papadopoulos, C.; Xu, J. Nanoelectronics: Growing Y-junction carbon nanotubes. *Nature* **1999**, *402*, 253–254. [CrossRef]
99. Nakayama, Y.; Zhang, M. Synthesis of carbon nanochaplets by catalytic thermal chemical vapor deposition. *Jpn. J. Appl. Phys.* **2001**, *40*, L492. [CrossRef]

100. De Heer, W.A.; Poncharal, P.; Berger, C.; Gezo, J.; Song, Z.; Bettini, J.; Ugarte, D. Liquid carbon, carbon-glass beads, and the crystallization of carbon nanotubes. *Science* **2005**, *307*, 907–910. [CrossRef] [PubMed]
101. Monthioux, M.; Allouche, H.; Jacobsen, R.L. Chemical vapour deposition of pyrolytic carbon on carbon nanotubes: Part 3: Growth mechanisms. *Carbon* **2006**, *44*, 3183–3194. [CrossRef]
102. Ting, J.-M.; Lan, J.B. Beaded carbon tubes. *Appl. Phys. Lett.* **1999**, *75*, 3309–3311. [CrossRef]
103. Sharma, P.; Ahuja, P. Recent advances in carbon nanotube-based electronics. *Mater. Res. Bull.* **2008**, *43*, 2517–2526. [CrossRef]
104. Wildoer, J.; Venema, L.; Rinzler, A.; Smalley, R.; Dekker, C. Electronic structure of carbon nanotubes investigated by scanning tunneling spectroscopy. *Nature* **1998**, *391*, 59–62.
105. Zhu, J.; Holmen, A.; Chen, D. Carbon nanomaterials in catalysis: Proton affinity, chemical and electronic properties, and their catalytic consequences. *ChemCatChem* **2013**, *5*, 378–401. [CrossRef]
106. Karami, M.; Bahabadi, M.A.; Delfani, S.; Ghozatloo, A. A new application of carbon nanotubes nanofluid as working fluid of low-temperature direct absorption solar collector. *Sol. Energy Mater. Sol. Cells* **2014**, *121*, 114–118. [CrossRef]
107. Esfe, M.H.; Saedodin, S.; Yan, W.-M.; Afrand, M.; Sina, N. Study on thermal conductivity of water-based nanofluids with hybrid suspensions of CNTs/Al_2O_3 nanoparticles. *J. Therm. Anal. Calorim.* **2016**, *124*, 455–460. [CrossRef]
108. Mauter, M.S.; Elimelech, M. Environmental applications of carbon-based nanomaterials. *Environ. Sci. Technol.* **2008**, *42*, 5843–5859. [CrossRef] [PubMed]
109. Thirumal, V.; Pandurangan, A.; Jayavel, R.; Krishnamoorthi, S.; Ilangovan, R. Synthesis of nitrogen doped coiled double walled carbon nanotubes by chemical vapor deposition method for supercapacitor applications. *Curr. Appl. Phys.* **2016**, *16*, 816–825. [CrossRef]
110. Hone, J. *Carbon Nanotube, Phonons and Thermal Properties*; Springer: Berlin/Heidelberg, Germany, 2001; Volume 80.
111. Robertson, D.; Brenner, D.; Mintmire, J. Energetics of nanoscale graphitic tubules. *Phys. Rev. B* **1992**, *45*, 12592. [CrossRef]
112. Yu, M.-F.; Files, B.S.; Arepalli, S.; Ruoff, R.S. Tensile loading of ropes of single wall carbon nanotubes and their mechanical properties. *Phys. Rev. Lett.* **2000**, *84*, 5552. [CrossRef] [PubMed]
113. Saifuddin, N.; Raziah, A.; Junizah, A. Carbon nanotubes: A review on structure and their interaction with proteins. *J. Chem.* **2012**, *2013*, 676815. [CrossRef]
114. Tans, S.J.; Verschueren, A.R.; Dekker, C. Room-temperature transistor based on a single carbon nanotube. *Nature* **1998**, *393*, 49–52. [CrossRef]
115. Bandyopadhyaya, R.; Nativ-Roth, E.; Regev, O.; Yerushalmi-Rozen, R. Stabilization of individual carbon nanotubes in aqueous solutions. *Nano Lett.* **2002**, *2*, 25–28. [CrossRef]
116. Kharissova, O.V.; Kharisov, B.I.; de Casas Ortiz, E.G. Dispersion of carbon nanotubes in water and non-aqueous solvents. *Rsc Adv.* **2013**, *3*, 24812–24852. [CrossRef]
117. Sondi, I.; Goia, D.V.; Matijević, E. Preparation of highly concentrated stable dispersions of uniform silver nanoparticles. *J. Colloid Interface Sci.* **2003**, *260*, 75–81. [CrossRef]
118. Yu, W.; Xie, H. A review on nanofluids: Preparation, stability mechanisms, and applications. *J. Nanomater.* **2012**, *2012*, 1. [CrossRef]
119. Bilalis, P.; Katsigiannopoulos, D.; Avgeropoulos, A.; Sakellariou, G. Non-covalent functionalization of carbon nanotubes with polymers. *Rsc Adv.* **2014**, *4*, 2911–2934. [CrossRef]
120. Sayes, C.M.; Liang, F.; Hudson, J.L.; Mendez, J.; Guo, W.; Beach, J.M.; Moore, V.C.; Doyle, C.D.; West, J.L.; Billups, W.E. Functionalization density dependence of single-walled carbon nanotubes cytotoxicity in vitro. *Toxicol. Lett.* **2006**, *161*, 135–142. [CrossRef] [PubMed]
121. Sehrawat, P.; Julien, C.; Islam, S.S. Carbon nanotubes in Li-ion batteries: A review. *Mater. Sci. Eng. B* **2016**, *213*, 12–40. [CrossRef]
122. Ma, L.; Hendrickson, K.E.; Wei, S.; Archer, L.A. Nanomaterials: Science and applications in the lithium–sulfur battery. *Nano Today* **2015**, *10*, 315–338. [CrossRef]
123. Shende, R.C.; Ramaprabhu, S. Thermo-optical properties of partially unzipped multiwalled carbon nanotubes dispersed nanofluids for direct absorption solar thermal energy systems. *Sol. Energy Mater. Sol. Cells* **2016**, *157*, 117–125. [CrossRef]

124. Muhammad, M.J.; Muhammad, I.A.; Sidik, N.A.C.; Yazid, M.N.A.W.M.; Mamat, R.; Najafi, G. The use of nanofluids for enhancing the thermal performance of stationary solar collectors: A review. *Renew. Sustain. Energy Rev.* **2016**, *63*, 226–236. [CrossRef]
125. Mesgari, S.; Taylor, R.A.; Hjerrild, N.E.; Crisostomo, F.; Li, Q.; Scott, J. An investigation of thermal stability of carbon nanofluids for solar thermal applications. *Sol. Energy Mater. Sol. Cells* **2016**, *157*, 652–659. [CrossRef]
126. Li, X.; Zou, C.; Chen, W.; Lei, X. Experimental investigation of β-cyclodextrin modified carbon nanotubes nanofluids for solar energy systems: Stability, optical properties and thermal conductivity. *Sol. Energy Mater. Sol. Cells* **2016**, *157*, 572–579. [CrossRef]
127. Dürkop, T.; Getty, S.; Cobas, E.; Fuhrer, M. Extraordinary mobility in semiconducting carbon nanotubes. *Nano Lett.* **2004**, *4*, 35–39. [CrossRef]
128. Wang, F.; Kozawa, D.; Miyauchi, Y.; Hiraoka, K.; Mouri, S.; Ohno, Y.; Matsuda, K. Considerably improved photovoltaic performance of carbon nanotube-based solar cells using metal oxide layers. *Nat. Commun.* **2015**, *6*, 6305. [CrossRef] [PubMed]
129. Alturaif, H.; ALOthman, Z.; Shapter, J.; Wabaidur, S. Use of carbon nanotubes (CNTs) with polymers in solar cells. *Molecules* **2014**, *19*, 17329–17344. [CrossRef] [PubMed]
130. Wei, J.; Jia, Y.; Shu, Q.; Gu, Z.; Wang, K.; Zhuang, D.; Zhang, G.; Wang, Z.; Luo, J.; Cao, A. Double-walled carbon nanotube solar cells. *Nano Lett.* **2007**, *7*, 2317–2321. [CrossRef] [PubMed]
131. Jia, Y.; Wei, J.; Wang, K.; Cao, A.; Shu, Q.; Gui, X.; Zhu, Y.; Zhuang, D.; Zhang, G.; Ma, B. Nanotube–silicon heterojunction solar cells. *Adv. Mater.* **2008**, *20*, 4594–4598. [CrossRef]
132. Liang, C.-W.; Roth, S. Electrical and optical transport of GaAs/carbon nanotube heterojunctions. *Nano Lett.* **2008**, *8*, 1809–1812. [CrossRef] [PubMed]
133. Signorelli, R.; Ku, D.C.; Kassakian, J.G.; Schindall, J.E. Electrochemical double-layer capacitors using carbon nanotube electrode structures. *Proc. IEEE* **2009**, *97*, 1837–1847. [CrossRef]
134. Xu, X.; Tan, H.; Xi, K.; Ding, S.; Yu, D.; Cheng, S.; Yang, G.; Peng, X.; Fakeeh, A.; Kumar, R.V. Bamboo-like amorphous carbon nanotubes clad in ultrathin nickel oxide nanosheets for lithium-ion battery electrodes with long cycle life. *Carbon* **2015**, *84*, 491–499. [CrossRef]
135. Wang, W.; Kumta, P.N. Nanostructured hybrid silicon/carbon nanotube heterostructures: Reversible high-capacity lithium-ion anodes. *ACS Nano* **2010**, *4*, 2233–2241. [CrossRef]
136. Wu, H.; Chan, G.; Choi, J.W.; Yao, Y.; McDowell, M.T.; Lee, S.W.; Jackson, A.; Yang, Y.; Hu, L.; Cui, Y. Stable cycling of double-walled silicon nanotube battery anodes through solid-electrolyte interphase control. *Nature Nanotechnol.* **2012**, *7*, 310–315. [CrossRef]
137. Xue, L.; Xu, G.; Li, Y.; Li, S.; Fu, K.; Shi, Q.; Zhang, X. Carbon-coated Si nanoparticles dispersed in carbon nanotube networks as anode material for lithium-ion batteries. *ACS Appl. Mater. Interfaces* **2012**, *5*, 21–25. [CrossRef] [PubMed]
138. Thepsuparungsikul, N.; Phonthamachai, N.; Ng, H. Multi-walled carbon nanotubes as electrode material for microbial fuel cells. *Water Sci. Technol.* **2012**, *65*, 1208–1214. [CrossRef] [PubMed]
139. Fraiwan, A.; Adusumilli, S.; Han, D.; Steckl, A.; Call, D.; Westgate, C.; Choi, S. Microbial Power-Generating Capabilities on Micro-/Nano-Structured Anodes in Micro-Sized Microbial Fuel Cells. *Fuel Cells* **2014**, *14*, 801–809. [CrossRef]
140. Ren, H.; Pyo, S.; Lee, J.-I.; Park, T.-J.; Gittleson, F.S.; Leung, F.C.; Kim, J.; Taylor, A.D.; Lee, H.-S.; Chae, J. A high power density miniaturized microbial fuel cell having carbon nanotube anodes. *J. Power Sources* **2015**, *273*, 823–830. [CrossRef]
141. Wang, Y.-Q.; Huang, H.-X.; Li, B.; Li, W.-S. Novelly developed three-dimensional carbon scaffold anodes from polyacrylonitrile for microbial fuel cells. *J. Mater. Chem. A* **2015**, *3*, 5110–5118. [CrossRef]
142. Xie, X.; Hu, L.; Pasta, M.; Wells, G.F.; Kong, D.; Criddle, C.S.; Cui, Y. Three-dimensional carbon nanotube−textile anode for high-performance microbial fuel cells. *Nano Lett.* **2011**, *11*, 291–296. [CrossRef] [PubMed]
143. Xie, X.; Ye, M.; Hu, L.; Liu, N.; McDonough, J.R.; Chen, W.; Alshareef, H.N.; Criddle, C.S.; Cui, Y. Carbon nanotube-coated macroporous sponge for microbial fuel cell electrodes. *Energy Environ. Sci.* **2012**, *5*, 5265–5270. [CrossRef]
144. He, Y.; Liu, Z.; Xing, X.-H.; Li, B.; Zhang, Y.; Shen, R.; Zhu, Z.; Duan, N. Carbon nanotubes simultaneously as the anode and microbial carrier for up-flow fixed-bed microbial fuel cell. *Biochem. Eng. J.* **2015**, *94*, 39–44. [CrossRef]

145. Shen, Y.; Zhou, Y.; Chen, S.; Yang, F.; Zheng, S.; Hou, H. Carbon nanofibers modified graphite felt for high performance anode in high substrate concentration microbial fuel cells. *Sci. World J.* **2014**, *2014*, 130185. [CrossRef]
146. Manickam, S.S.; Karra, U.; Huang, L.; Bui, N.-N.; Li, B.; McCutcheon, J.R. Activated carbon nanofiber anodes for microbial fuel cells. *Carbon* **2013**, *53*, 19–28. [CrossRef]
147. Pokhrel, L.R.; Ettore, N.; Jacobs, Z.L.; Zarr, A.; Weir, M.H.; Scheuerman, P.R.; Kanel, S.R.; Dubey, B. Novel carbon nanotube (CNT)-based ultrasensitive sensors for trace mercury(II) detection in water: A review. *Sci. Total Environ.* **2017**, *574*, 1379–1388. [CrossRef] [PubMed]
148. Anitha, K.; Namsani, S.; Singh, J.K. Removal of Heavy Metal Ions Using a Functionalized Single-Walled Carbon Nanotube: A Molecular Dynamics Study. *J. Phys. Chem. A* **2015**, *119*, 8349–8358. [CrossRef] [PubMed]
149. Tofighy, M.A.; Mohammadi, T. Nickel ions removal from water by two different morphologies of induced CNTs in mullite pore channels as adsorptive membrane. *Ceram. Int.* **2015**, *41*, 5464–5472. [CrossRef]
150. Zhu, X.; Cui, Y.; Chang, X.; Wang, H. Selective solid-phase extraction and analysis of trace-level Cr (III), Fe (III), Pb (II), and Mn (II) Ions in wastewater using diethylenetriamine-functionalized carbon nanotubes dispersed in graphene oxide colloids. *Talanta* **2016**, *146*, 358–363. [CrossRef] [PubMed]
151. Mubarak, N.M.; Sahu, J.N.; Abdullah, E.C.; Jayakumar, N.S. Rapid adsorption of toxic Pb (II) ions from aqueous solution using multiwall carbon nanotubes synthesized by microwave chemical vapor deposition technique. *J. Environ. Sci.* **2016**, *45*, 143–155. [CrossRef] [PubMed]
152. Li, Y.-H.; Wang, S.; Wei, J.; Zhang, X.; Xu, C.; Luan, Z.; Wu, D.; Wei, B. Lead adsorption on carbon nanotubes. *Chem. Phys. Lett.* **2002**, *357*, 263–266. [CrossRef]
153. Lu, C.; Liu, C. Removal of nickel (II) from aqueous solution by carbon nanotubes. *J. Chem. Technol. Biotechnol.* **2006**, *81*, 1932–1940. [CrossRef]
154. Abbas, A.; Al-Amer, A.M.; Laoui, T.; Al-Marri, M.J.; Nasser, M.S.; Khraisheh, M.; Atieh, M.A. Heavy metal removal from aqueous solution by advanced carbon nanotubes: Critical review of adsorption applications. *Sep. Purif. Technol.* **2016**, *157*, 141–161.
155. Santhosh, C.; Velmurugan, V.; Jacob, G.; Jeong, S.K.; Grace, A.N.; Bhatnagar, A. Role of nanomaterials in water treatment applications: A review. *Chem. Eng. J.* **2016**, *306*, 1116–1137. [CrossRef]
156. Wu, C.-H. Adsorption of reactive dye onto carbon nanotubes: Equilibrium, kinetics and thermodynamics. *J. Hazard. Mater.* **2007**, *144*, 93–100. [CrossRef]
157. Bahgat, M.; Farghali, A.A.; El Rouby, W.M.A.; Khedr, M.H. Synthesis and modification of multi-walled carbon nano-tubes (MWCNTs) for water treatment applications. *J. Anal. Appl. Pyrolysis* **2011**, *92*, 307–313. [CrossRef]
158. Cano, O.A.; González, C.R.; Paz, J.H.; Madrid, P.A.; Casillas, P.G.; Hernández, A.M.; Pérez, C.M. Catalytic activity of palladium nanocubes/multiwalled carbon nanotubes structures for methyl orange dye removal. *Catal. Today* **2017**, *282*, 168–173. [CrossRef]
159. Ma, J.; Yu, F.; Zhou, L.; Jin, L.; Yang, M.; Luan, J.; Tang, Y.; Fan, H.; Yuan, Z.; Chen, J. Enhanced adsorptive removal of methyl orange and methylene blue from aqueous solution by alkali-activated multiwalled carbon nanotubes. *ACS Appl. Mater. Interfaces* **2012**, *4*, 5749–5760. [CrossRef] [PubMed]
160. Wang, S.; Ng, C.W.; Wang, W.; Li, Q.; Hao, Z. Synergistic and competitive adsorption of organic dyes on multiwalled carbon nanotubes. *Chem. Eng. J.* **2012**, *197*, 34–40. [CrossRef]
161. Lou, J.C.; Jung, M.J.; Yang, H.W.; Han, J.Y.; Huang, W.H. Removal of dissolved organic matter (DOM) from raw water by single-walled carbon nanotubes (SWCNTs). *J. Environ. Sci. Health Part A* **2011**, *46*, 1357–1365. [CrossRef] [PubMed]
162. Zhu, H.; Jiang, R.; Xiao, L.; Zeng, G. Preparation, characterization, adsorption kinetics and thermodynamics of novel magnetic chitosan enwrapping nanosized γ-Fe_2O_3 and multi-walled carbon nanotubes with enhanced adsorption properties for methyl orange. *Bioresour. Technol.* **2010**, *101*, 5063–5069. [CrossRef] [PubMed]
163. Yang, W.; Lu, Y.; Zheng, F.; Xue, X.; Li, N.; Liu, D. Adsorption behavior and mechanisms of norfloxacin onto porous resins and carbon nanotube. *Chem. Eng. J.* **2012**, *179*, 112–118. [CrossRef]
164. Ncibi, M.C.; Sillanpää, M. Optimized removal of antibiotic drugs from aqueous solutions using single, double and multi-walled carbon nanotubes. *J. Hazard. Mater.* **2015**, *298*, 102–110. [CrossRef]
165. Yang, Q.; Chen, G.; Zhang, J.; Li, H. Adsorption of sulfamethazine by multi-walled carbon nanotubes: Effects of aqueous solution chemistry. *Rsc Adv.* **2015**, *5*, 25541–25549. [CrossRef]

166. Fard, A.K.; Mckay, G.; Manawi, Y.; Malaibari, Z.; Hussien, M.A. Outstanding adsorption performance of high aspect ratio and super-hydrophobic carbon nanotubes for oil removal. *Chemosphere* **2016**, *164*, 142–155. [CrossRef]
167. Qiu, W.; Xu, H.; Takalkar, S.; Gurung, A.S.; Liu, B.; Zheng, Y.; Guo, Z.; Baloda, M.; Baryeh, K.; Liu, G. Carbon nanotube-based lateral flow biosensor for sensitive and rapid detection of DNA sequence. *Biosens. Bioelectron.* **2015**, *64*, 367–372. [CrossRef] [PubMed]
168. Sinha, N.; Yeow, J.-W. Carbon nanotubes for biomedical applications. *IEEE Trans. NanoBiosci.* **2005**, *4*, 180–195. [CrossRef]
169. Joseph, H. MEMS in the medical world. *Sens. J. Appl. Sens. Technol.* **1997**, *14*, 47–51.
170. Bernal-Martínez, J.; Seseña-Rubfiaro, A.; Godínez-Fernández, R.; Aguilar-Elguezabal, A. Electrodes made of multi-wall carbon nanotubes on PVDF-filters have low electrical resistance and are able to record electrocardiograms in humans. *Microelectron. Eng.* **2016**, *166*, 10–14. [CrossRef]
171. Vohrer, U.; Kolaric, I.; Haque, M.; Roth, S.; Detlaff-Weglikowska, U. Carbon nanotube sheets for the use as artificial muscles. *Carbon* **2004**, *42*, 1159–1164. [CrossRef]
172. Zeng, Z.; Jin, H.; Zhang, L.; Zhang, H.; Chen, Z.; Gao, F.; Zhang, Z. Low-voltage and high-performance electrothermal actuator based on multi-walled carbon nanotube/polymer composites. *Carbon* **2015**, *84*, 327–334. [CrossRef]
173. Foroughi, J.; Spinks, G.M.; Aziz, S.; Mirabedini, A.; Jeiranikhameneh, A.; Wallace, G.G.; Kozlov, M.E.; Baughman, R.H. Knitted carbon-nanotube-sheath/spandex-core elastomeric yarns for artificial muscles and strain sensing. *ACS Nano* **2016**, *10*, 9129–9135. [CrossRef] [PubMed]
174. Inganäs, O.; Lundström, I. Carbon nanotube muscles. *Science* **1999**, *284*, 1281–1282.
175. Wu, L.; Qu, X. Cancer biomarker detection: Recent achievements and challenges. *Chem. Soc. Rev.* **2015**, *44*, 2963–2997. [CrossRef]
176. Hong, H.; Gao, T.; Cai, W. Molecular imaging with single-walled carbon nanotubes. *Nano Today* **2009**, *4*, 252–261. [CrossRef]
177. Patel, A.; Prajapati, P.; Chaudhari, K.; Boghra, R.; Jadhav, A. Carbon nanotubes production, characterisation and its applications. *J. Adv. Pharm. Sci.* **2010**, *1*, 187–195.
178. Marquis, F.D. Fully integrated hybrid polymeric carbon nanotube composites. In *Materials Science Forum*; Trans Tech Publications Ltd.: Zurich-Uetikon, Switzerland, 2003; Volume 437, pp. 85–88.
179. Bian, Z.; Wang, R.J.; Wang, W.H.; Zhang, T.; Inoue, A. Carbon-Nanotube-Reinforced Zr-Based Bulk Metallic Glass Composites and Their Properties. *Adv. Funct. Mater.* **2004**, *14*, 55–63. [CrossRef]
180. Costa, P.M.; Bourgognon, M.; Wang, J.T.; Al-Jamal, K.T. Functionalised carbon nanotubes: From intracellular uptake and cell-related toxicity to systemic brain delivery. *J. Control. Release* **2016**, *241*, 200–219. [CrossRef] [PubMed]
181. Flahaut, E.; Rul, S.; Lefévre-Schlick, F.; Laurent, C.; Peigney, A. Carbon Nanotubes-Ceramic Composites. *Ceram. Nanomater. Nanotechnol. II* **2004**, *148*, 69–82.
182. Yanagi, H.; Kawai, Y.; Kita, T.; Fujii, S.; Hayashi, Y.; Magario, A.; Noguchi, T. Carbon nanotube/aluminum composites as a novel field electron emitter. *Jpn. J. Appl. Phys.* **2006**, *45*, L650. [CrossRef]
183. Baughman, R.H.; Cui, C.; Zakhidov, A.A.; Iqbal, Z.; Barisci, J.N.; Spinks, G.M.; Wallace, G.G.; Mazzoldi, A.; De Rossi, D.; Rinzler, A.G. Carbon nanotube actuators. *Science* **1999**, *284*, 1340–1344. [CrossRef] [PubMed]
184. Niu, C.; Sichel, E.K.; Hoch, R.; Moy, D.; Tennent, H. High power electrochemical capacitors based on carbon nanotube electrodes. *Appl. Phys. Lett.* **1997**, *70*, 1480–1482. [CrossRef]
185. Dai, H.; Hafner, J.H.; Rinzler, A.G.; Colbert, D.T.; Smalley, R.E. Nanotubes as nanoprobes in scanning probe microscopy. *Nature* **1996**, *384*, 147–150. [CrossRef]
186. Tibbetts, G.G.; Meisner, G.P.; Olk, C.H. Hydrogen storage capacity of carbon nanotubes, filaments, and vapor-grown fibers. *Carbon* **2001**, *39*, 2291–2301. [CrossRef]
187. Wei, J.; Zhu, H.; Wu, D.; Wei, B. Carbon nanotube filaments in household light bulbs. *Appl. Phys. Lett.* **2004**, *84*, 4869–4871. [CrossRef]
188. Yu, X.; Munge, B.; Patel, V.; Jensen, G.; Bhirde, A.; Gong, J.D.; Kim, S.N.; Gillespie, J.; Gutkind, J.S.; Papadimitrakopoulos, F. Carbon nanotube amplification strategies for highly sensitive immunodetection of cancer biomarkers. *J. Am. Chem. Soc.* **2006**, *128*, 11199–11205. [CrossRef] [PubMed]

189. Okuno, J.; Maehashi, K.; Kerman, K.; Takamura, Y.; Matsumoto, K.; Tamiya, E. Label-free immunosensor for prostate-specific antigen based on single-walled carbon nanotube array-modified microelectrodes. *Biosens. Bioelectron.* **2007**, *22*, 2377–2381. [CrossRef] [PubMed]
190. Ou, C.; Yuan, R.; Chai, Y.; Tang, M.; Chai, R.; He, X. A novel amperometric immunosensor based on layer-by-layer assembly of gold nanoparticles–multi-walled carbon nanotubes-thionine multilayer films on polyelectrolyte surface. *Anal. Chim. Acta* **2007**, *603*, 205–213. [CrossRef] [PubMed]
191. Kim, J.P.; Lee, B.Y.; Lee, J.; Hong, S.; Sim, S.J. Enhancement of sensitivity and specificity by surface modification of carbon nanotubes in diagnosis of prostate cancer based on carbon nanotube field effect transistors. *Biosens. Bioelectron.* **2009**, *24*, 3372–3378. [CrossRef] [PubMed]
192. Bi, S.; Zhou, H.; Zhang, S. Multilayers enzyme-coated carbon nanotubes as biolabel for ultrasensitive chemiluminescence immunoassay of cancer biomarker. *Biosens. Bioelectron.* **2009**, *24*, 2961–2966. [CrossRef] [PubMed]
193. Liu, C.-H.; Wu, C.-C.; Zhong, Z. A fully tunable single-walled carbon nanotube diode. *Nano Lett.* **2011**, *11*, 1782–1785. [CrossRef] [PubMed]
194. Lee, J.U. Photovoltaic effect in ideal carbon nanotube diodes. *Appl. Phys. Lett.* **2005**, *87*, 073101. [CrossRef]
195. Jilili, J.; Abdurahman, A.; Gülseren, O.; Schwingenschlögl, U. Non-covalent functionalization of single wall carbon nanotubes and graphene by a conjugated polymer. *Appl. Phys. Lett.* **2014**, *105*, 013103. [CrossRef]
196. Chen, C.; Jin, T.; Wei, L.; Li, Y.; Liu, X.; Wang, Y.; Zhang, L.; Liao, C.; Hu, N.; Song, C. High-work-function metal/carbon nanotube/low-work-function metal hybrid junction photovoltaic device. *NPG Asia Mater.* **2015**, *7*, e220. [CrossRef]
197. Miyata, Y.; Shiozawa, K.; Asada, Y.; Ohno, Y.; Kitaura, R.; Mizutani, T.; Shinohara, H. Length-sorted semiconducting carbon nanotubes for high-mobility thin film transistors. *Nano Res.* **2011**, *4*, 963–970. [CrossRef]
198. Martel, R.; Derycke, V.; Appenzeller, J.; Wind, S.; Avouris, P. Carbon nanotube field-effect transistors and logic circuits. In Proceedings of the 39th Annual Design Automation Conference, New Orleans, LA, USA, 10–14 June 2002; pp. 94–98.
199. Peng, L.-M.; Zhang, Z.; Wang, S. Carbon nanotube electronics: Recent advances. *Mater. Today* **2014**, *17*, 433–442. [CrossRef]
200. Appenzeller, J.; Martel, R.; Avouris, P.; Stahl, H.; Lengeler, B. Optimized contact configuration for the study of transport phenomena in ropes of single-wall carbon nanotubes. *Appl. Phys. Lett.* **2001**, *78*, 3313–3315. [CrossRef]
201. Chen, Z.; Appenzeller, J.; Knoch, J.; Lin, Y.-m.; Avouris, P. The role of metal−nanotube contact in the performance of carbon nanotube field-effect transistors. *Nano Lett.* **2005**, *5*, 1497–1502. [CrossRef] [PubMed]
202. Sinha, N.; Ma, J.; Yeow, J.T. Carbon nanotube-based sensors. *J. Nanosci. Nanotechnol.* **2006**, *6*, 573–590. [CrossRef] [PubMed]
203. Jacobs, C.B.; Peairs, M.J.; Venton, B.J. Carbon nanotube based electrochemical sensors for biomolecules. *Anal. Chim. Acta* **2010**, *662*, 105–127. [CrossRef] [PubMed]
204. Yang, N.; Chen, X.; Ren, T.; Zhang, P.; Yang, D. Carbon nanotube based biosensors. *Sens. Actuators B Chem.* **2015**, *207*, 690–715. [CrossRef]
205. Zhu, Z.; Song, W.; Burugapalli, K.; Moussy, F.; Li, Y.-L.; Zhong, X.-H. Nano-yarn carbon nanotube fiber based enzymatic glucose biosensor. *Nanotechnology* **2010**, *21*, 165501. [CrossRef]
206. Fatoni, A.; Numnuam, A.; Kanatharana, P.; Limbut, W.; Thammakhet, C.; Thavarungkul, P. A highly stable oxygen-independent glucose biosensor based on a chitosan-albumin cryogel incorporated with carbon nanotubes and ferrocene. *Sens. Actuators B Chem.* **2013**, *185*, 725–734. [CrossRef]
207. Kan, X.; Zhou, H.; Li, C.; Zhu, A.; Xing, Z.; Zhao, Z. Imprinted electrochemical sensor for dopamine recognition and determination based on a carbon nanotube/polypyrrole film. *Electrochim. Acta* **2012**, *63*, 69–75. [CrossRef]
208. Wang, Y.; Yeow, J.T. A review of carbon nanotubes-based gas sensors. *J. Sens.* **2009**, *2009*, 493904. [CrossRef]
209. Jeong, H.Y.; Lee, D.-S.; Choi, H.K.; Lee, D.H.; Kim, J.-E.; Lee, J.Y.; Lee, W.J.; Kim, S.O.; Choi, S.-Y. Flexible room-temperature NO_2 gas sensors based on carbon nanotubes/reduced graphene hybrid films. *Appl. Phys. Lett.* **2010**, *96*, 213105. [CrossRef]
210. Abdulla, S.; Mathew, T.L.; Pullithadathil, B. Highly sensitive, room temperature gas sensor based on polyaniline-multiwalled carbon nanotubes (PANI/MWCNTs) nanocomposite for trace-level ammonia detection. *Sens. Actuators B Chem.* **2015**, *221*, 1523–1534. [CrossRef]

211. Saito, Y.; Uemura, S. Field emission from carbon nanotubes and its application to electron sources. *Carbon* **2000**, *38*, 169–182. [CrossRef]
212. Lee, N.; Chung, D.; Han, I.; Kang, J.; Choi, Y.; Kim, H.; Park, S.; Jin, Y.; Yi, W.; Yun, M. Application of carbon nanotubes to field emission displays. *Diamond Relat. Mater.* **2001**, *10*, 265–270. [CrossRef]
213. De Heer, W.A.; Chatelain, A.; Ugarte, D. A carbon nanotube field-emission electron source. *Science* **1995**, *270*, 1179–1181. [CrossRef]
214. Rosen, R.; Simendinger, W.; Debbault, C.; Shimoda, H.; Fleming, L.; Stoner, B.; Zhou, O. Application of carbon nanotubes as electrodes in gas discharge tubes. *Appl. Phys. Lett.* **2000**, *76*, 1668–1670. [CrossRef]
215. Sugie, H.; Tanemura, M.; Filip, V.; Iwata, K.; Takahashi, K.; Okuyama, F. Carbon nanotubes as electron source in an X-ray tube. *Appl. Phys. Lett.* **2001**, *78*, 2578–2580. [CrossRef]
216. Neupane, S.; Lastres, M.; Chiarella, M.; Li, W.; Su, Q.; Du, G. Synthesis and field emission properties of vertically aligned carbon nanotube arrays on copper. *Carbon* **2012**, *50*, 2641–2650. [CrossRef]
217. Huang, Z.; Carnahan, D.; Rybczynski, J.; Giersig, M.; Sennett, M.; Wang, D.; Wen, J.; Kempa, K.; Ren, Z. Growth of large periodic arrays of carbon nanotubes. *Appl. Phys. Lett.* **2003**, *82*, 460–462. [CrossRef]
218. Teo, K.; Lee, S.; Chhowalla, M.; Semet, V.; Binh, V.T.; Groening, O.; Castignolles, M.; Loiseau, A.; Pirio, G.; Legagneux, P. Plasma enhanced chemical vapour deposition carbon nanotubes/nanofibres—How uniform do they grow? *Nanotechnology* **2003**, *14*, 204. [CrossRef]
219. Kim, D.-H.; Cho, D.-S.; Jang, H.-S.; Kim, C.-D.; Lee, H.-R. The growth of freestanding single carbon nanotube arrays. *Nanotechnology* **2003**, *14*, 1269. [CrossRef] [PubMed]
220. Wu, J.; Eastman, M.; Gutu, T.; Wyse, M.; Jiao, J.; Kim, S.-M.; Mann, M.; Zhang, Y.; Teo, K. Fabrication of carbon nanotube-based nanodevices using a combination technique of focused ion beam and plasma-enhanced chemical vapor deposition. *Appl. Phys. Lett.* **2007**, *91*, 173122. [CrossRef]
221. Lee, C.J.; Kim, D.W.; Lee, T.J.; Choi, Y.C.; Park, Y.S.; Lee, Y.H.; Choi, W.B.; Lee, N.S.; Park, G.-S.; Kim, J.M. Synthesis of aligned carbon nanotubes using thermal chemical vapor deposition. *Chem. Phys. Lett.* **1999**, *312*, 461–468. [CrossRef]
222. Dionne, M.; Coulombe, S.; Meunier, J.-L. Screening effects between field-enhancing patterned carbon nanotubes: A numerical study. *IEEE Trans. Electron Devices* **2008**, *55*, 1298–1305. [CrossRef]
223. Wright, A.W. ART. VII.—On the production of Transparent Metallic Films by the Electrical Discharge in exhausted tubes. *Am. J. Sci. Arts* **1877**, *13*, 49. [CrossRef]
224. Baedeker, K. Über die elektrische Leitfähigkeit und die thermoelektrische Kraft einiger Schwermetallverbindungen. *Ann. Phys.* **1907**, *327*, 749–766. [CrossRef]
225. Hecht, D.S.; Hu, L.; Irvin, G. Emerging transparent electrodes based on thin films of carbon nanotubes, graphene, and metallic nanostructures. *Adv. Mater.* **2011**, *23*, 1482–1513. [CrossRef]
226. Kolosov, O.; Gruverman, A.; Hatano, J.; Takahashi, K.; Tokumoto, H. Nanoscale visualization and control of ferroelectric domains by atomic force microscopy. *Phys. Rev. Lett.* **1995**, *74*, 4309. [CrossRef]
227. Lanza, M.; Bayerl, A.; Gao, T.; Porti, M.; Nafria, M.; Jing, G.; Zhang, Y.; Liu, Z.; Duan, H. Graphene-Coated Atomic Force Microscope Tips for Reliable Nanoscale Electrical Characterization. *Adv. Mater.* **2013**, *25*, 1440–1444. [CrossRef]
228. Stevens, R.M. New carbon nanotube AFM probe technology. *Mater. Today* **2009**, *12*, 42–45. [CrossRef]
229. Slattery, A.D.; Shearer, C.J.; Gibson, C.T.; Shapter, J.G.; Lewis, D.A.; Stapleton, A.J. Carbon nanotube modified probes for stable and high sensitivity conductive atomic force microscopy. *Nanotechnology* **2016**, *27*, 475708. [CrossRef] [PubMed]
230. Slattery, A.D.; Blanch, A.J.; Quinton, J.S.; Gibson, C.T. Efficient attachment of carbon nanotubes to conventional and high-frequency AFM probes enhanced by electron beam processes. *Nanotechnology* **2013**, *24*, 235705. [CrossRef] [PubMed]
231. Wang, S.; Haldane, D.; Liang, R.; Smithyman, J.; Zhang, C.; Wang, B. Nanoscale infiltration behaviour and through-thickness permeability of carbon nanotube buckypapers. *Nanotechnology* **2012**, *24*, 015704. [CrossRef] [PubMed]
232. Li, Y.; Kröger, M. A theoretical evaluation of the effects of carbon nanotube entanglement and bundling on the structural and mechanical properties of buckypaper. *Carbon* **2012**, *50*, 1793–1806. [CrossRef]
233. He, S.; Wei, J.; Guo, F.; Xu, R.; Li, C.; Cui, X.; Zhu, H.; Wang, K.; Wu, D. A large area, flexible polyaniline/buckypaper composite with a core–shell structure for efficient supercapacitors. *J. Mater. Chem. A* **2014**, *2*, 5898–5902. [CrossRef]

234. Lu, H.; Gou, J. Study on 3-D high conductive graphene buckypaper for electrical actuation of shape memory polymer. *Nanosci. Nanotechnol. Lett.* **2012**, *4*, 1155–1159. [CrossRef]
235. Che, J.; Chen, P.; Chan-Park, M.B. High-strength carbon nanotube buckypaper composites as applied to free-standing electrodes for supercapacitors. *J. Mater. Chem. A* **2013**, *1*, 4057–4066. [CrossRef]
236. Liu, Q.; Nayfeh, M.H.; Yau, S.-T. Brushed-on flexible supercapacitor sheets using a nanocomposite of polyaniline and carbon nanotubes. *J. Power Sources* **2010**, *195*, 7480–7483. [CrossRef]
237. Chen, I.-W.P.; Yang, M.-C.; Yang, C.-H.; Zhong, D.-X.; Hsu, M.-C.; Chen, Y. Newton Output Blocking Force under Low-Voltage Stimulation for Carbon Nanotube–Electroactive Polymer Composite Artificial Muscles. *ACS Appl. Mater. Interfaces* **2017**, *9*, 5550–5555. [CrossRef]
238. Schwengber, A.; Prado, H.J.; Zilli, D.A.; Bonelli, P.R.; Cukierman, A.L. Carbon nanotubes buckypapers for potential transdermal drug delivery. *Mater. Sci. Eng. C* **2015**, *57*, 7–13. [CrossRef]
239. Aqil, A.; Vlad, A.; Piedboeuf, M.-L.; Aqil, M.; Job, N.; Melinte, S.; Detrembleur, C.; Jérôme, C. A new design of organic radical batteries (ORBs): Carbon nanotube buckypaper electrode functionalized by electrografting. *Chem. Commun.* **2015**, *51*, 9301–9304. [CrossRef] [PubMed]
240. Giubileo, F.; Iemmo, L.; Luongo, G.; Martucciello, N.; Raimondo, M.; Guadagno, L.; Passacantando, M.; Lafdi, K.; Di Bartolomeo, A. Transport and field emission properties of buckypapers obtained from aligned carbon nanotubes. *J. Mater. Sci.* **2017**, *52*, 6459–6468. [CrossRef]
241. Wu, Q.; Zhu, W.; Zhang, C.; Liang, Z.; Wang, B. Study of fire retardant behavior of carbon nanotube membranes and carbon nanofiber paper in carbon fiber reinforced epoxy composites. *Carbon* **2010**, *48*, 1799–1806. [CrossRef]
242. Yang, X.; Lee, J.; Yuan, L.; Chae, S.-R.; Peterson, V.K.; Minett, A.I.; Yin, Y.; Harris, A.T. Removal of natural organic matter in water using functionalised carbon nanotube buckypaper. *Carbon* **2013**, *59*, 160–166. [CrossRef]
243. Rashid, M.H.-O.; Pham, S.Q.; Sweetman, L.J.; Alcock, L.J.; Wise, A.; Nghiem, L.D.; Triani, G.; in het Panhuis, M.; Ralph, S.F. Synthesis, properties, water and solute permeability of MWNT buckypapers. *J. Membr. Sci.* **2014**, *456*, 175–184. [CrossRef]
244. Wen, G.; Yu, H.; Huang, X. Synthesis of carbon microtube buckypaper by a gas pressure enhanced chemical vapor deposition method. *Carbon* **2011**, *49*, 4067–4069. [CrossRef]
245. LeMieux, M.C.; Roberts, M.; Barman, S.; Jin, Y.W.; Kim, J.M.; Bao, Z. Self-sorted, aligned nanotube networks for thin-film transistors. *Science* **2008**, *321*, 101–104. [CrossRef] [PubMed]
246. Khan, Z.U.; Kausar, A.; Ullah, H.; Badshah, A.; Khan, W.U. A review of graphene oxide, graphene buckypaper, and polymer/graphene composites: Properties and fabrication techniques. *J. Plast. Film Sheeting* **2016**, *32*, 336–379. [CrossRef]